
**GEOLOGICAL SURVEY OF CANADA**
**OPEN FILE 7358**

# Portable XRF spectrometry of reference materials with respect to precision, accuracy, instrument drift, dwell time optimization, and calibration.

**R.D. Knight, B.A. Kjarsgaard, A.P. Plourde, M. Moroz**

**2013**

Natural Resources Canada | Ressources naturelles Canada

Canada


**GEOLOGICAL SURVEY OF CANADA**
**OPEN FILE 7358**

# Portable XRF spectrometry of reference materials with respect to precision, accuracy, instrument drift, dwell time optimization, and calibration.

**R.D. Knight, B.A. Kjarsgaard, A.P. Plourde, M. Moroz**

**2013**



doi:10.4095/292677
This publication is available for free download through GEOSCAN (http://geoscan.ess.nrcan.gc.ca/).

**Recommended citation**
Knight, R.D., Kjarsgaard, B.A., Plourde, A.P., and Moroz, M., 2013. Portable XRF spectrometry of standard reference materials with respect to precision, accuracy, instrument drift, dwell time optimization, and calibration; Geological Survey of Canada, Open File 7358. doi:10.4095/292677

Publications in this series have not been edited; they are released as submitted by the author.

## Table of Contents

1.0 Introduction .....1

1.1 Background information for analysed materials.....2
1.1 Methods .....5

2.0 Instrument Drift .....10

2.1 Daily Drift .....10
2.2 Drift over extended time periods .....13
2.3 Summary of instrument drift .....14

3.0 Effect of dwell time .....15

3.1 Possible effects of detector saturation .....23
3.2 Summary of dwell time effects .....24

4.0 Element interference .....24

5.0 Examining calibrations .....29

5.1 Factory and post-collection calibrations .....33
5.2 Categorising elements based on results from Till-1, -2, -3, and -4 .....35

6.0 Conclusion .....38

Acknowledgments.....39

References.....40

## 1.0 Introduction

Over the last decade the use of portable X-ray fluorescence (pXRF) spectrometers for both environmental and exploration geochemistry has grown significantly. Several studies have examined precision, accuracy and calibration of pXRF spectrometers for the examination of rocks (e.g. Weltje and Tjallingii, 2008; Morris, 2009; Gazley et al., 2011; Rowe et al., 2012) and soils (e.g., Kenna et al., 2011; McLaren et al., 2011; Weindorf et al., 2012). At the Geological Survey of Canada (GSC), pXRF spectrometers have also been successfully used to characterize aquitard chemostratigraphy within the Groundwater Geoscience Program (Crow et al., 2012; Knight et al., 2012; Plourde et al., 2012), to characterize eruptive phases of a kimberlite in the James Bay lowlands (Grunsky et al., 2013), and to characterize surficial sediments in the Thelon River area, Northwest Territories (Plourde et al., 2013). However, other than Morris (2009), the precision and accuracy of reference materials by pXRF has received comparatively little attention, despite the importance of these materials in the proper calibration of these instruments. Knight et al. (2012) examined the precision and accuracy of two similar pXRF spectrometers while undertaking a chemostratigraphic study of the silt and clay size fraction within a Champlain Sea aquitard. For that study pXRF data were compared with geochemical analyses obtained by fusion digestion coupled with ICP-ES/MS analysis and concluded that with careful analytical protocols pXRF is a viable method to define the chemostratigraphy of fine grained sediments. One outcome was to group elements into classes based on the reproducibility of the pXRF data as compared to the fusion data (Fig. 1). Subsequently, Plourde et al. (2012) undertook a study that compared pXRF data from both in-situ and processed aquitard sediment obtained from a borehole within the Spiritwood buried valley, southwest Manitoba. They concluded that pXRF spectrometry does not provide meaningful results for sediment with abundant pebbles and variable grain sizes. However, removal of size fractions greater than 0.063 mm provided highly improved results that could be used in conjunction with both visual core logging and downhole geophysical methods to assist in the interpretation of the borehole stratigraphy.

For this study, a total of 4749 analyses were carried out to examine the precision and accuracy of a pXRF spectrometer. Samples analysed included:

1.) CANMET certified reference materials: Till-1, -2, -3, and -4
2.) National Institute for Standards and Technology: NIST 610, NIST 2780 glasses
3.) Geological Survey of Canada internal till standard TCA 8010
4.) Resource Conservation and Recovery Act: RCRA 180-436, NCS 73308
5.) Multi-element standards DLH 7, DLH 10b
6.) $SiO_2$ blank

Results and discussions are divided into four sections and address instrument drift, dwell time effects, element interference examples, and calibration.

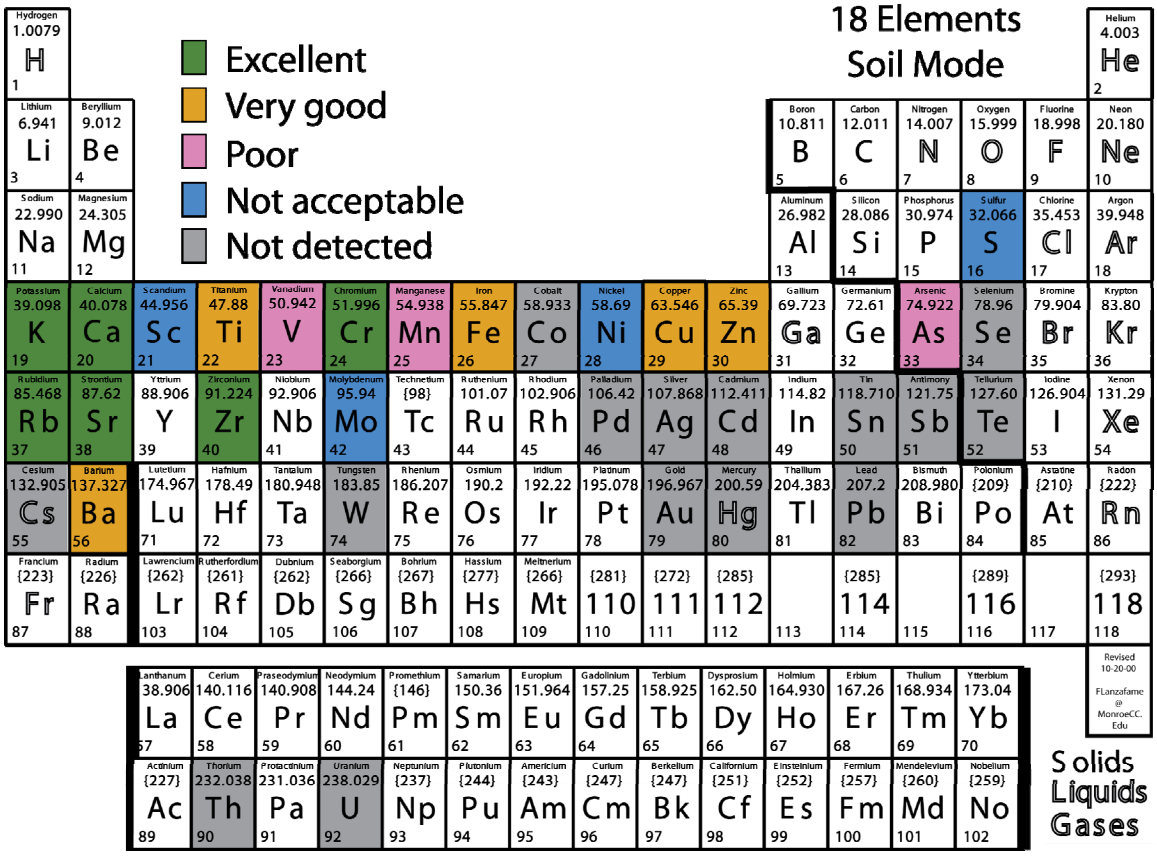


Figure 1. Summary of the elements detected pXRF spectrometers in Soil Mode for fine-grained sediments from the Champlain Sea near Kinburn, Ontario (after Knight et al 2012).

### 1.1 Background information for analysed materials

In 1996, John Lynch, a research scientist with the Geological Survey of Canada, published a report on the analyses of four surficial sediment samples that became standard reference materials (SRM) at the Geological Survey of Canada for exploration and environmental studies. These samples are identified as Till-1, -2, -3, and -4. Till-1 was collected 25 km northwest of Lanark, Ontario near Joe Lake. Till-2 was collected 5 km west of Sisson Brook, New Brunswick. Till-3 was collected 8 km east of Cobalt, Ontario, near the O'Brien mine. Till-4 was principally collected in Sisson Brook, New Brunswick, however some molybdenite bearing soil from near Gatineau, Quebec was blended with the till prior to analyses in order to raise the molybdenum content (Lynch**,** 1996). Till-1 and Till-3 are soil samples, whereas Till-2 and Till-4 represent glacial derived till. These samples cover a broad range of concentrations and are representative of glacial derived materials sourced from several different bedrock types within Canada. A partial list of elemental composition is listed in Table 1, whereas a complete list is presented in Lynch (1996). The four reference samples all contain a silica matrix, with $SiO_2$ concentration of 60.9 wt%, 60.8 wt%, 69.1 wt%, and 65.0 wt%, respectively (Lynch, 1996).

| Element | Till-1 | | Till-2 | | Till-3 | | Till-4 | |
|---|---|---|---|---|---|---|---|---|
| | C (ppm) | σ (ppm) | C (ppm) | σ (ppm) | C (ppm) | σ (ppm) | C (ppm) | σ (ppm) |
| **As** | 18 | 1 | 26 | 2 | 87 | 4 | 111 | 6 |
| **Ba** | 702 | 59 | 540 | 56 | 489 | 36 | 395 | 37 |
| **Ca** | 19440 | 715 | 9077 | 500 | 18797 | 715 | 8934 | 357 |
| **Co** | 18 | 2 | 15 | 2 | 15 | 2 | 8 | 2 |
| **Cr** | 65 | 6 | 74 | 8 | 123 | 14 | 53 | 10 |
| **Cs** | 1 | 0.2 | 12 | 1 | 1.7 | 0.4 | 12 | 1 |
| **Cu** | 47 | 4 | 150 | 10 | 22 | 5 | 237 | 17 |
| **Fe** | 48100 | 2200 | 38400 | 1700 | 27800 | 1200 | 39700 | 1900 |
| **K** | 18429 | 830 | 25486 | 996 | 20090 | 830 | 26980 | 996 |
| **Mn** | 1420 | 75 | 780 | 28 | 520 | 39 | 490 | 30 |
| **Mo** | 2 | 1 | 14 | 2 | 2 | 1 | 16 | 2 |
| **Ni** | 24 | 4 | 32 | 3 | 39 | 7 | 17 | 3 |
| **Pb** | 22 | 3 | 31 | 3 | 26 | 3 | 50 | 4 |
| **Rb** | 44 | 6 | 143 | 12 | 55 | 7 | 161 | 15 |
| **S** | < 500 | | < 500 | | < 500 | | 800 | 100 |
| **Sb** | 7.8 | 0.5 | 0.8 | 0.1 | 0.9 | 0.1 | 1 | 0.1 |
| **Sc** | 13 | 2 | 12 | 0.1 | 10 | 1 | 10 | 1 |
| **Sr** | 291 | 10 | 144 | 8 | 300 | 12 | 109 | 11 |
| **Th** | 5.6 | 0.5 | 18.4 | 1.4 | 4.6 | 0.4 | 17.4 | 1.4 |
| **Ti** | 5990 | 210 | 5300 | 190 | 2910 | 90 | 4840 | 130 |
| **U** | 2.2 | 0.3 | 5.7 | 0.4 | 2.1 | 0.2 | 5 | 0.5 |
| **V** | 99 | 10 | 77 | 10 | 62 | 6 | 67 | 7 |
| **W** | <1 | | 5 | 1 | <1 | | 204 | 24 |
| **Zn** | 98 | 10 | 130 | 8 | 56 | 6 | 70 | 7 |
| **Zr** | 502 | 58 | 390 | 39 | 230 | 24 | 385 | 34 |

Table 1. Certified elemental concentrations and standard deviations determined by numerous laboratories, for the Till series (Lynch, 1996). Only elements detected by the pXRF are included in this table. C = concentration; σ = one standard deviation.

DLH 7 and DLH 10b are silicate glass standards produced at the Pilkington Glass research laboratory in conjunction with the University of Manchester. Hamilton and Hopkins (1995) provide details of their preparation. DLH 10b was subsequently crushed into a powder that was used in this study. DLH 7 elemental concentrations where determined by three independent laboratories using laser ablation ICP-MS. Concentrations listed in Table 2 are a mean of the obtained results. DLH 10b elemental concentrations were measured by ICP-MS following a single acid dissolution of two pieces of glass from two different melt castings with analysis performed at the University of Manchester (Hamilton and Hopkins, 1995). Element concentrations for glass standards DLH7 and DLH10b are listed in Table 2, as well as new data recently acquired at the Geological Survey of Canada by the laser ablation ICP-MS method.

| Element | DLH 7 | DLH 10b | NIST 610 | NIST 2780 | NCS 73308 | RCRA 180-436 | TCA 8010 | $SiO_2$ blank |
|---|---|---|---|---|---|---|---|---|
| As | .51 | 3.52 | 340* | 48.8 | | 500 | 5.45# | |
| Ba | 64.5 | 900 (970) | 453 | 993 | 42 | 500 | 549 | |
| Ca | 85331 | 76067 | 81500 | 1950 | 2800 | | 15509 | Trace |
| Cd | | | 244 | 12.1 | | 500 | 0.11# | |
| Co | 64.3 (68) | 919 (1017) | *244*** | | | | 7.9 | |
| Cr | 51.8 (60) | 173 (374) | 408 | 44 | 136 | 500 | 48.4 | |
| Cs | | | | | | | 1 | |
| Cu | 64.2 (69) | 527 (869) | (444)** | 215 | 23 | | 28 | Trace |
| Fe | 90.6 | 70.9 | 458 | 27840 | 2700 | | 20290 | Trace |
| K | 91.1 (56) | 26.1 | *461* | 33800 | 1041 | | 19094 | |
| Mn | 69.5 (67) | 1008 (1027) | 457 | 462 | 1010 | | 310 | |
| Mo | 56.8 (62) | 204 (312) | *417* | | | | .7 | |
| Ni | 67.4 (62) | 928 (963) | 459 | | | | 17.2 | |
| Pb | 44.8 (64) | 25.4 (85) | 426 | 5770 | 27 | 500 | 12.2 | |
| Rb | (67) | (945) | 426 | | 9.2 | | 53.6 | |
| Sb | | | 415 | | | | 2.30# | Trace |
| Sc | 68.6 (67) | 959 (968) | *455* | | | | 9.2 | |
| Se | 3.21 | <.2 | 115 | | | 500 | 0.23#* | |
| Sn | | | *430* | | | | 0.6 | |
| Sr | (72) | (1073) | 516 | | 25 | | 310 | |
| Te | | | | | | | 0.02#* | |
| Th | <.01 | <.01 | 457 | | | | 5.1 | |
| Ti | 1.16 | 930 (1019) | *437* | | 1270 | | 2578 | Trace |
| U | 70.7 (75) | <1 | 462 | | | | 1.1 | |
| V | 67.4 (72) | 906 (1295) | 450 | | 107 | | 49 | |
| W | (79) | (252) | *444* | | | | 0.5 | |
| Zn | 70.2 (62) | 890 (932) | *433* | 2570 | 46 | | 31.9 | Trace |
| Zr | 67.9 (72) | 910 (884) | *448* | | 70 | | 272 | Trace |

For NIST 610 and NIST 2780
* Certified Value in regular font
** Reference value in brackets
*** Information only value in italics font

Table 2. Elemental concentrations for the DLH 7, DLH 10b, NIST 610, NIST 2780, RCRA 180-436, TCA 810 and a $SiO_2$ blank. For DLH 7 and DLH 10, values are from LA-ICP-MS (mean 10 spots; Kjarsgaard, unpublished); values in brackets are from Hamilton and Hopkins (1995). Data for TCA8010 is the mean of 39 analyses (Kjarsgaard, in press) by fusion digestion and ICP-ES/MS analysis. For TCA8010, all data from fusion, except # by 4 acid; #* by aqua regia.

NIST 610 is a Standard Reference Material (SRM) glass produced by the National Institute for Standards and Technology (NIST) in the United States (Pearce et al., 1997). It contains up to sixty-one trace elements at a nominal concentration level of 500 ppm. The recommended concentrations listed in Appendix B are from the recent study of Jochum et al. (2011) that involved laser ablation ICP-MS carried out a 2 different laboratories, ICP-MS following a dissolution in HF-$HNO_3$ at $160^0$C for 3 days, evaporation and redissolution in aqua-regia, then HCL, and using the wavelength-dispersive detection mode of a Jeol JXA-8200 electron microprobe with a acceleration voltage of 15kV and beam current of 12nA. Appendix B also includes data from the original NIST Certificate of Analyses. Hinton (2007) provides an overview of the manufacture methods for the glass standard and suggests that the glass, although returning slightly lower concentrations levels than originally reported by NIST, are as homogeneous as indicated by NIST.

NIST 2780 is a powder of hard rock mine waste from the Silverton Mining District, Colorado, and is often used as a standard for test materials that possess significant heavy metal concentrations. Wilson et al (1999) provides a brief overview of the collection, preparation and testing of the original NIST 2780 sample material and concludes that this standard reference material is homogeneous.

Resource Conservation and Recovery Act (RCRA) 180-436 and processed soil sediment NCS 73308 are standards supplied with the pXRF by Thermo Scientific. Although pXRF spectrometry measures a large suite of elements, only six elements (see Table 2) are reported as recommended values for RCRA 180-436 (As, Ba, Cd, Cr, Pb and Se). The pXRF operation manual provided by Thermo Scientific states that RCRA 180-436 is not a true SRM as values have not been confirmed and places a ± value of 100 ppm on detected concentrations. NCS 73308 replaces NIST 2709, which is a low element concentration standard that is no longer available.

TCA 8010 is a till sample from southern Manitoba, subsequently powdered and utilized as an 'in-house' GSC standard reference material. Available data from aqua-regia and total fusion digestion analyses are reported in Girard et al. (2004) and Kjarsgaard et al. (in press).

Certified, recommended, and reference concentrations relevant to pXRF analysis for NIST 610, NIST 2780, DLH 7, DLH 10b, RCRA 180-436, TCA 810, and an $SiO_2$ blank are listed in Table 2.

### 1.2 Methods

Data were acquired using a handheld Thermo Scientific Niton XL3t GOLDD XRF spectrometer equipped with a Cygnet 50 kV, 2 watt, Ag Anode X-ray tube and a XL3 silicon drift detector (SDD) with 180,000 counts per second (cps) throughput, which was mounted in a test stand (Fig. 2). A summary of the number of analyses per sample, dwell times per filter and sample material are presented in Tables 3 to 7. Most pXRF spectrometers offer analyses in three modes; 1) Test all GEO Mode, where the expected elemental concentration is unknown by the user, 2) Mining Mode, where expected elemental concentration is >1%, and 3) Soil Mode, where the expected

concentration is <1%. All analyses were carried out in Soil Mode. All reference materials were analysed with 60 second dwell times for each of the Main, Low, and High filters, for a total of 180 seconds per analysis (Table 3).


Figure 2. The Niton pXRF mounted in a test stand.

| Reference material | Material type | Number of analyses | Main Filter (s) | Low Filter (s) | High Filter (s) | Total Time (s) |
|---|---|---|---|---|---|---|
| Till-1 | Powder | 106 | 60 | 60 | 60 | 180 |
| Till-2 | Powder | 106 | 60 | 60 | 60 | 180 |
| Till-3 | Powder | 106 | 60 | 60 | 60 | 180 |
| Till-4 | Powder | 129 | 60 | 60 | 60 | 180 |
| NIST 610 | Glass | 111 | 60 | 60 | 60 | 180 |
| NIST 2780 | Powder | 35 | 60 | 60 | 60 | 180 |
| DLH 7 | Glass | 148 | 60 | 60 | 60 | 180 |
| DLH 10b | Powder from glass | 115 | 60 | 60 | 60 | 180 |
| NCS 73308 | Powder | 45 | 60 | 60 | 60 | 180 |
| RCRA | Powder | 85 | 60 | 60 | 60 | 180 |
| TCA 8010 | Powder | 163 | 60 | 60 | 60 | 180 |
| SiO2 | Powder | 82 | 60 | 60 | 60 | 180 |

Table 3. Number of analyses and material type for twelve reference materials at 60 s dwell time per filter.

In addition, Till-1, NIST 610, DLH 7, and DLH 10b were analysed with a dwell time of 5, 10, 20, 30, 40, 50, and 60 seconds for the Main (50 kv @ 40 µA max), Low (20 kv @ 100 µA max), and High (50 kv @ 40 µA max) filters (Tables 4, 5, 6, and 7). NIST 610, DLH 7 and DLH 10b were also analysed with a dwell time of 70 and 80 seconds for the Main and Low filters (Tables 5, 6, and 7). A list of the filters and spectral lines used for each element is presented in Table 8.

Till-1, Till-2, Till-3, DLH 7, DLH 10b, NIST 610, and TCA 8010 were analysed repeatedly (continuously) over a short period of time in order to examine potential drift in the resulting measurements. Data for Till-4, NIST 2780, NCS 73308 and RCRA 180-436 were collected for quality control purposes throughout multiple studies over a four year period (e.g., Knight et al., 2012; Plourde et al., 2012; Grunsky et al., 2013). Powdered standards were covered by a SpectroCertified® Mylar® polyester sheet, whereas glass standards were placed directly on the test stand. Note that Soil Mode, utilizing Compton normalization, was used for the entirety of this study despite potential matrix differences between silicate glass standards (DLH 7, DLH 10b, and NIST 610) and soils.

A $SiO_2$ blank was used to monitor the cleanliness of the pXRF window and sample stand environment. Over the course of the study, the majority of $SiO_2$ blank analyses returned trace concentrations of elements (e.g., Ca and Fe) as impurities in the SpectroCertified® Mylar® polyester. Some elements (e.g., K and Cs) are not listed as known impurities, but were also detected in small amounts. For three analyses, the $SiO_2$ blank returned anomalous values for a number of elements, suggesting that the test stand was contaminated. Cleaning the stand using a light stream of air returned the detection to normal Mylar® polyester impurity levels.

| Reference material | Number of analyses | Main Filter (s) | Low Filter (s) | High Filter (s) | Total Time (s) |
|---|---|---|---|---|---|
| Till-1 | 120 | 5 | 5 | 5 | 15 |
| Till-1 | 107 | 10 | 10 | 10 | 30 |
| Till-1 | 105 | 20 | 20 | 20 | 60 |
| Till-1 | 109 | 30 | 30 | 30 | 90 |
| Till-1 | 78 | 40 | 40 | 40 | 120 |
| Till-1 | 106 | 60 | 60 | 60 | 180 |
| Till-1 | 105 | 70 | 70 | 0 | 140 |

Table 4. Number of analyses, dwell time per filter, and total dwell time for Till-1.

| Reference material | Number of analyses | Main Filter (s) | Low Filter (s) | High Filter (s) | Total Time (s) |
|---|---|---|---|---|---|
| NIST 610 | 171 | 5 | 5 | 5 | 15 |
| NIST 610 | 115 | 10 | 10 | 10 | 30 |
| NIST 610 | 116 | 20 | 20 | 20 | 60 |
| NIST 610 | 112 | 30 | 30 | 30 | 90 |
| NIST 610 | 104 | 40 | 40 | 40 | 120 |
| NIST 610 | 176 | 50 | 50 | 50 | 150 |
| NIST 610 | 111 | 60 | 60 | 60 | 180 |
| NIST 610 | 105 | 70 | 70 | 40 | 180 |
| NIST 610 | 117 | 80 | 80 | 20 | 180 |

Table 5. Number of analyses, dwell time per filter, and total dwell time for NIST 610.

| Reference material | Number of analyses | Main Filter (s) | Low Filter (s) | High Filter (s) | Total Time (s) |
|---|---|---|---|---|---|
| DLH 7 | 112 | 5 | 5 | 5 | 15 |
| DLH 7 | 116 | 10 | 10 | 10 | 30 |
| DLH 7 | 110 | 20 | 20 | 20 | 60 |
| DLH 7 | 112 | 30 | 30 | 30 | 90 |
| DLH 7 | 115 | 40 | 40 | 40 | 120 |
| DLH 7 | 115 | 50 | 50 | 50 | 150 |
| DLH 7 | 148 | 60 | 60 | 60 | 180 |
| DLH 7 | 104 | 70 | 70 | 0 | 140 |
| DLH 7 | 105 | 80 | 80 | 0 | 160 |

Table 6. Number of analyses, dwell time per filter, and total dwell time for DLH 7.

| Reference material | Number of analyses | Main Filter (s) | Low Filter (s) | High Filter (s) | Total Time (s) |
|---|---|---|---|---|---|
| DLH 10b | 116 | 5 | 5 | 5 | 15 |
| DLH 10b | 117 | 10 | 10 | 10 | 30 |
| DLH 10b | 115 | 20 | 20 | 20 | 60 |
| DLH 10b | 116 | 30 | 30 | 30 | 90 |
| DLH 10b | 162 | 40 | 40 | 40 | 120 |
| DLH 10b | 113 | 50 | 50 | 50 | 150 |
| DLH 10b | 115 | 60 | 60 | 60 | 180 |
| DLH 10b | 111 | 70 | 70 | 0 | 140 |
| DLH 10b | 105 | 80 | 80 | 0 | 160 |

Table 7. Number of analyses, dwell time per filter, and total dwell time for DLH 10b.

| Element | Line | Energy (keV) | Window Low (keV) | Window High (keV) | Filter |
|---|---|---|---|---|---|
| As | $K\alpha_1$ | 10.54 | 10.33 | 10.73 | Main |
| Ba | $K\alpha_1$ | 32.19 | 31.70 | 32.70 | High |
| Ca | $K\alpha_1$ | 3.69 | 3.50 | 3.89 | Low |
| Cd | $K\alpha_1$ | 23.17 | 22.60 | 23.60 | High |
| Co | $K\alpha_1$ | 6.93 | 6.73 | 7.13 | Main |
| Cr | $K\alpha_1$ | 5.41 | 5.24 | 5.59 | Low |
| Cs | $K\alpha_1$ | 30.97 | 29.50 | 31.50 | High |
| Cu | $K\alpha_1$ | 8.05 | 7.84 | 8.24 | Main |
| Fe | $K\alpha_1$ | 6.40 | 6.20 | 6.60 | Main |
| Hg | $L\alpha_1$ | 9.99 | 9.79 | 10.18 | Main |
| K | $K\alpha_1$ | 3.31 | 3.10 | 3.49 | Low |
| Mn | $K\alpha_1$ | 5.90 | 5.70 | 6.10 | Main |
| Mo | $K\alpha_1$ | 17.48 | 17.23 | 17.68 | Main |
| Ni | $K\alpha_1$ | 7.48 | 7.35 | 7.67 | Main |
| Pb | $L\beta_1$ | 12.61 | 12.40 | 12.80 | Main |
| Rb | $K\alpha_1$ | 13.39 | 13.18 | 13.60 | Main |
| S | $K\alpha_1$ | 2.31 | 2.20 | 2.45 | Low |
| Sb | $K\alpha_1$ | 26.36 | 25.90 | 26.90 | High |
| Sc | $K\alpha_1$ | 4.09 | 3.90 | 4.19 | Low |
| Se | $K\alpha_1$ | 11.22 | 11.01 | 11.41 | Main |
| Sn | $K\alpha_1$ | 25.27 | 24.70 | 25.70 | High |
| Sr | $K\alpha_1$ | 14.16 | 13.95 | 14.38 | Main |
| Te | $K\alpha_1$ | 27.47 | 27.00 | 28.00 | High |
| Th | $L\alpha_1$ | 12.97 | 12.80 | 13.15 | Main |
| Ti | $K\alpha_1$ | 4.51 | 4.21 | 4.70 | Low |
| U | $L\alpha_1$ | 13.61 | 13.48 | 13.90 | Main |
| V | $K\alpha_1$ | 4.95 | 4.80 | 5.10 | Low |
| W | $L\alpha_1$ | 8.40 | 8.26 | 8.49 | Main |
| Zn | $K\alpha_1$ | 8.64 | 8.49 | 8.83 | Main |
| Zr | $K\alpha_1$ | 15.77 | 15.53 | 15.98 | Main |

Table 8. X-ray energy emission lines used to determine elemental concentrations in Soil Mode, as provided by Niton.

## 2.0 Instrument Drift

The data sets containing results of the pXRF analyses are presented in Appendix A. Appendix B contains plots of the analytical results for elements detected consistently during the analyses. Each graph depicts the measured concentration as a blue solid circle, with smaller red solid circles indicating ± 2 standard deviations (2σ). Solid vertical lines on the graphs represent a period of time when the spectrometer was turned off overnight, whereas dashed vertical lines represent time breaks of ≥30 minutes between analyses carried out during a single day. Recommended values for each element (Tables 1 and 2) are indicated in the bottom right hand corner of the graph, and if the recommended value plots within the y-axis limits they are represented on the graphs by a dashed horizontal line. Plots for Till-4 do not include vertical lines to indicate time breaks since these analyses were collected over multiple studies for quality control during analysis (Appendix B).

### 2.1 Daily drift

For exploration and environmental studies, pXRF data are often collected at numerous sites throughout a day. Continuous analysis of reference materials provides information on instrument drift, instrument performance, and the state and stability of the X-ray tube and detector.

Pb is an example of an element for which measurements did not vary with time. In Till-1, 106 measurements with a dwell time of 60 seconds were obtained over a two-day period. The mean concentration was 23 ppm, slightly higher than the recommended value of 22 ppm (Fig. 3). The relative standard deviation (RSD), the typical measure of precision, was 9.4%. Of the 106 analyses, only three returned values outside the +/-2σ limits of 19-28 ppm (Appendix A). Plots for As, Ba, Cr, Cu, Mn, V, and Zn are similar, and display elemental concentration measurements that are variable, but within +/- 2σ of the mean (Appendix B).

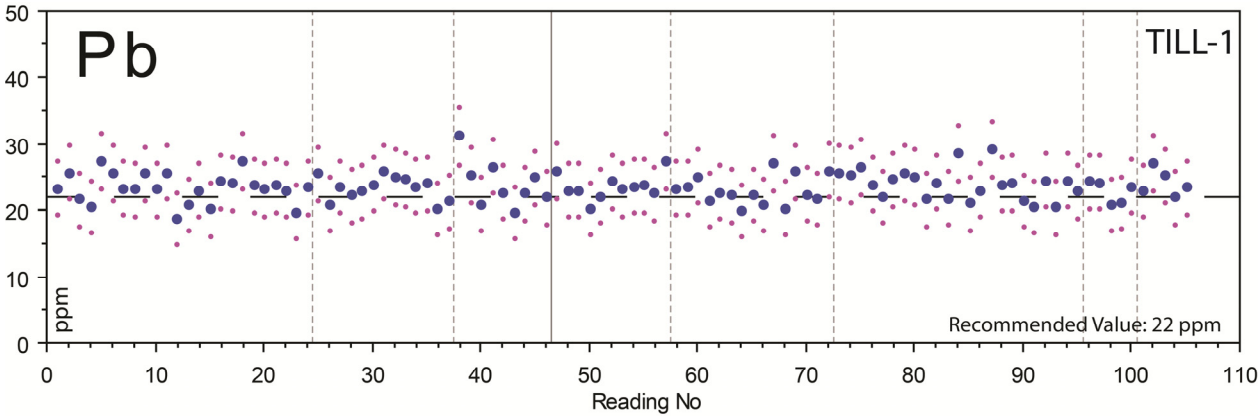


Figure 3. Pb analyses for Till-1 with a dwell time of 60 seconds per filter.

Figure 4 depicts of U data acquired for samples Till-2 and NIST 610 glass standard. For Till-2, 102 analyses of U were completed over a three-day period with a range in values of 6–22 ppm and RSD of 30% (see Appendix A); the recommended value is 5.7 ppm (Table 1). A single analysis (#1) for Till-2 was collected approximately one month prior to the others and is much higher than the rest of the data. The first vertical dashed line located at analysis #44 (Fig. 4) represents a 30 minute break before completing the data collection on that day. Not indicated on Figure 4 are time breaks of 10 and 16 minutes, respectively, at analyses #28 and #35. It should be noted that the measurements of U in Till-2 are mostly below 20 ppm and sometimes below 10 ppm; a 4 ppm limit of detection for the pXRF spectrometer is reported by Niton for a $SiO_2$+Fe+Ca matrix sample (Thermo Scientific, 2008).

For NIST 610, 111 analyses were acquired over a three-day period with a range in U values from 442–543 ppm and a RSD of 2.8% (see Appendix A); the recommended value is 462 ppm (Table 2). For Till-2 and NIST 610, U measurements increased with time until they were "reset" to lower values after a 30 to 90 minute time break between analyses. These results suggest that instrument drift occurred over the course of U analysis and may provide insight into more subtle differences in measured concentrations of other elements.

Till-2 exhibits increasing U measurements from analysis #2 to #33, followed by a decrease until analysis #44. Although more subtle, Ti, Ca, and K display a similar trend between analyses #2 through #44 (Fig. 5). At analyses #68 there is a day break with a large shift in the U measurements and minor shifts in Ti, Ca, and K. Less pronounced shifts would be difficult to correct for via calibration. However, with U being an exception, these fluctuations are small in terms of percent difference, and would likely be insignificant relative to inter-sample differences of a study. For example, the well defined drop of K measurements measured in Till-2 between analyses #68 and #69, represents only a small (~2%) decrease.

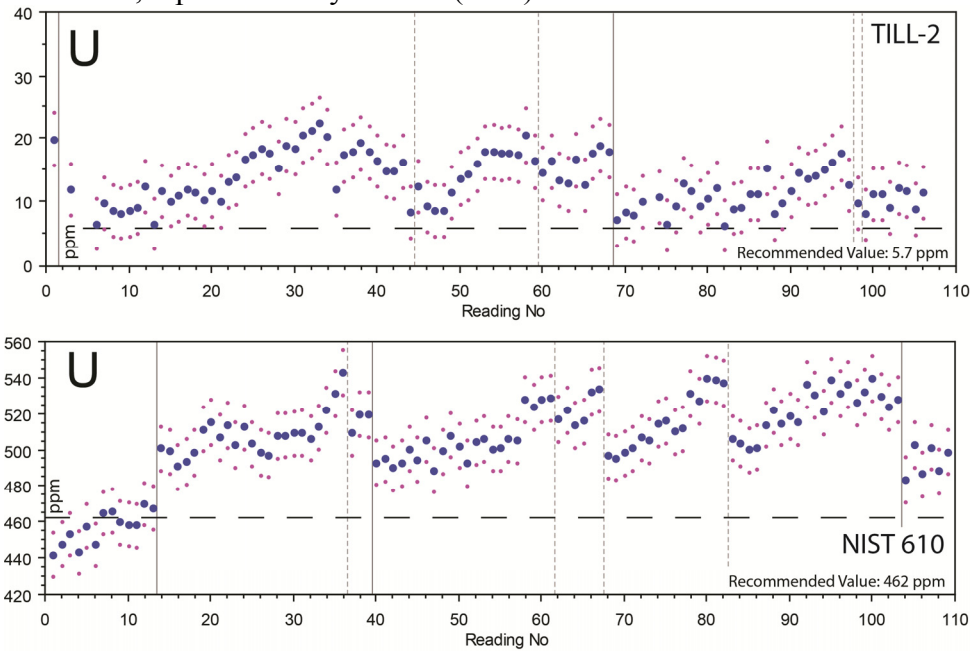


Figure 4. Uranium analyses for Till-2 and NIST 610 with a dwell time of 60 seconds per filter.

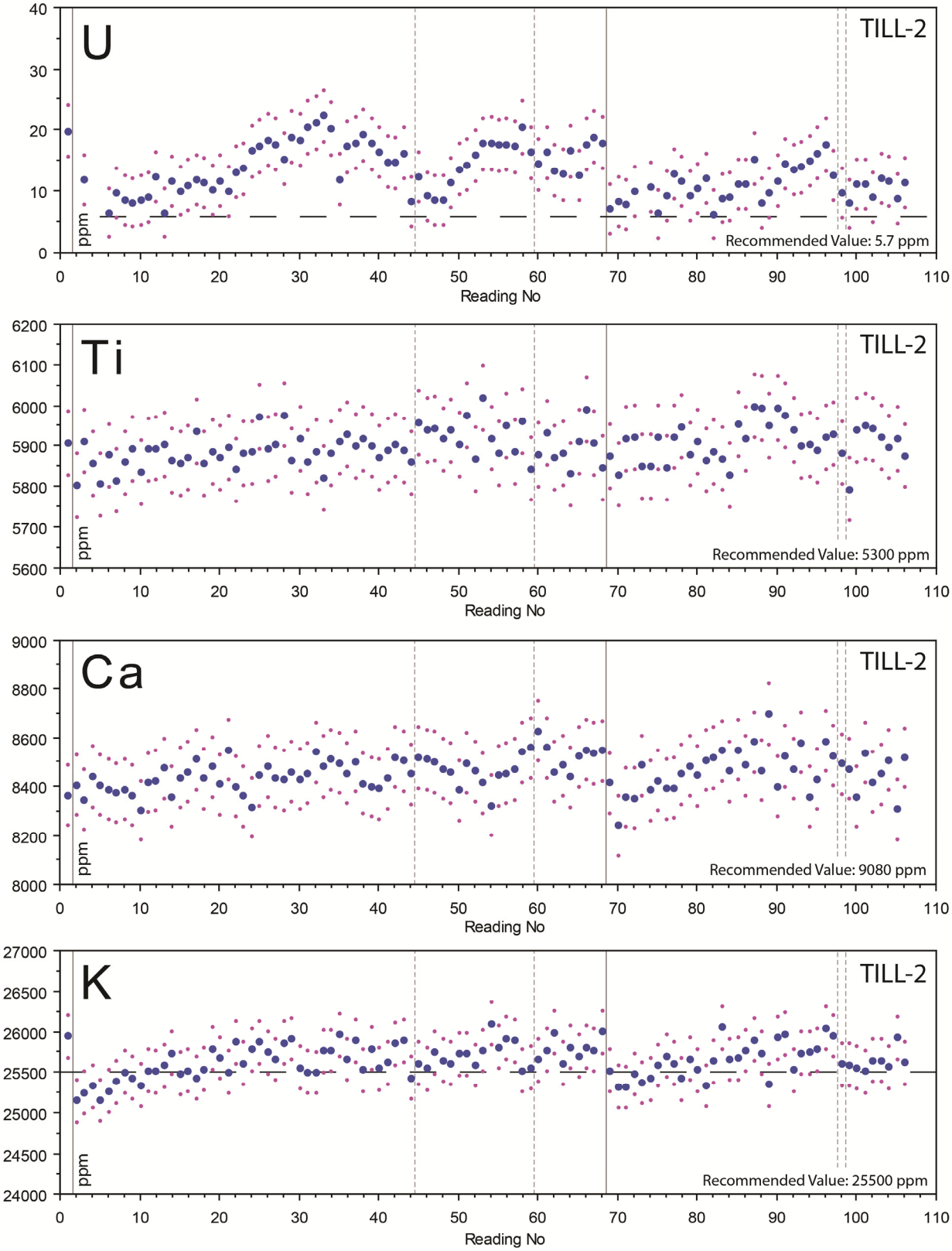


Figure 5. U, Ti, Ca, and K analyses for Till-2 with a dwell time of 60 seconds per filter.

## 2.2 Drift over extended time periods

Measurements obtained for Zr from Till-2 and Till-4 are displayed in Figure 6. For both reference materials all measurements are higher than the recommended values (displayed as a dashed horizontal line). For Till-2 there is little evidence of any instrument drift over the first day (analyses #2 through #68). The initial reading, which is considerably higher than any subsequent reading, was obtained over one month before the remaining analyses (Fig. 6). Although this is an individual analysis, the measured Zr concentration is outside the acceptable degree of uncertainty (± 2σ) compared to the 106 analyses collected over a two-day period. The remaining measurements show minor variation, with individual measurements within the uncertainty of ± 2σ. Readings obtained on the second day of analyses (#69 through #107) continue to be similar (within ± 2σ of each other), until analysis #98 (Appendix A) when the Zr measurements decrease from 415 ppm to 408 ppm, then to 405 ppm and 400 ppm (± 2σ of 9 ppm).

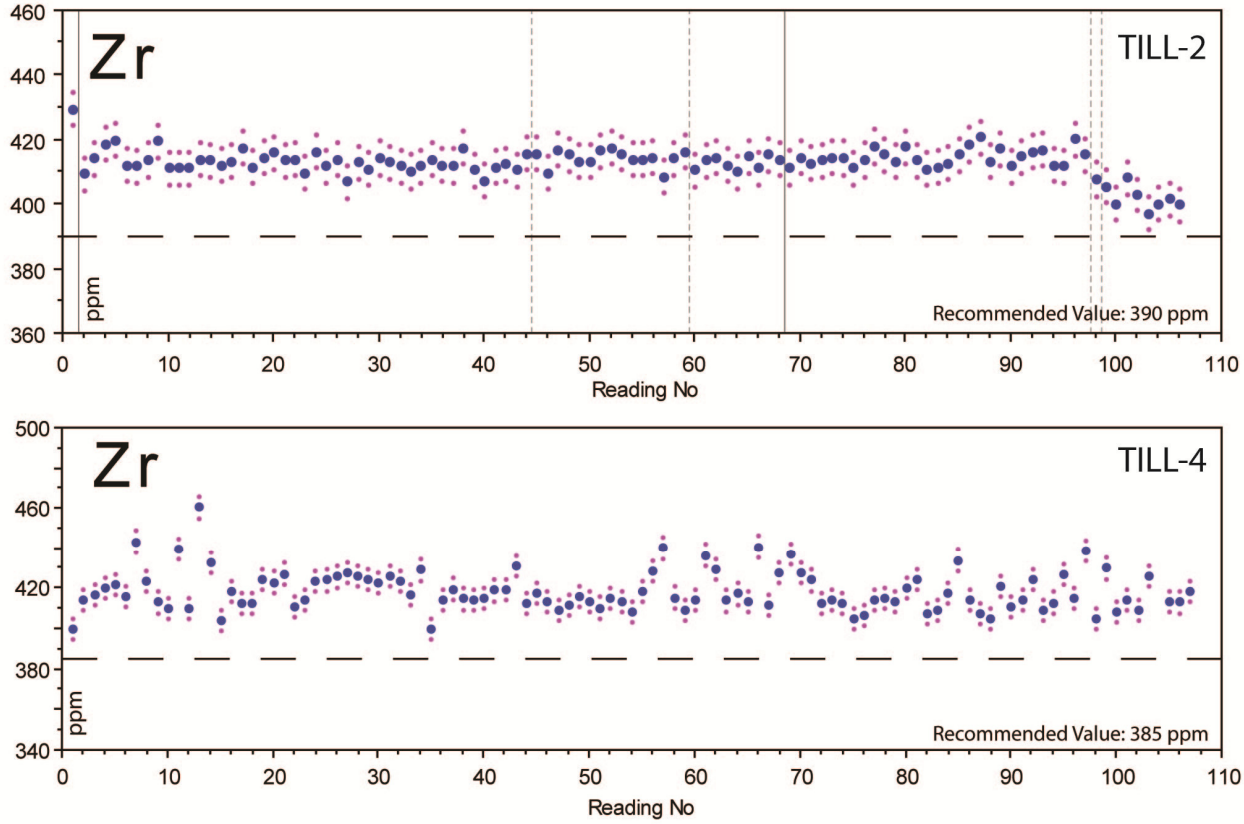


Figure 6. Zr analyses for Till-2 and Till-4 with a dwell time of 60 seconds per filter.

Data for Till-4 were collected from several studies as a quality control standard. Figure 6 displays the results of 106 measurements of Zr collected on 27 different days, over an 8 month period; on any given day there may have been hours between repeat analyses (see Appendix A for date and time of analyses). The data vary between 400 and 461 ppm. The tenth value in the dataset of 306 ppm was removed as all the data from this analysis is erroneous (see Appendix A). There are

several anomalous values that are much higher than the value obtained immediately before and after, as shown for reading #7 with a concentration of 443 ppm compared to adjacent values at 416 ppm and 424 ppm. K and Ca data obtained for Till-4 (see Appendix B) do display some systematic groupings where similar measurements are obtained on a single day. Most elements, however, do not display clear evidence for systematic instrument drift over long periods of time.

### 2.3 Summary of instrument drift

The above examples illustrate that data, collected in isolation over long time intervals (months), may be difficult to interpret. This in effect decreases the precision of the instrument for some elements (e.g., Ca, K, and Ti), as compared to a study completed over a short time period. Table 9 summarizes the elements that exhibit little to no drift, minor drift, and potentially significant drift, as determined from analyses of NIST 610, DLH 7, DLH 10b, Till-1, -2, -3, and -4 reference materials. Instrument drift over a lengthy study period will affect the precision of the obtained results especially if analytical conditions also vary over the study period.

Reference material analyses collected before, during, and after regular sample analyses provides quality assurance to monitor potential analytical drift. In addition, comparing reference material analyses with previously determined concentrations provides a foundation for deciding if post-collection data calibration is necessary.

| Elements that may exhibit significant drift | Elements that exhibit minor drift | Elements that exhibit little to no drift |
|---|---|---|
| Ca | Ba | As |
| Fe | Co | Cs |
| K | Cr | Ni |
| Ti | Cu | Pb |
| U | Mn | Rb |
| | Mo | Sr |
| | Zr | Th |
| | | V |
| | | W |
| | | Zn |

Table 9. List of elements that display significant, minor, or no drift in concentration over time.

## 3.0 Effect of dwell time

The ability to quantify and effectively eliminate instrument background from the sample signal is a limiting factor in all analytical methods. For pXRF spectrometry, instrumental background effects (brehmsstrahlung) can be assessed by extending analytical dwell time. Data collection below a "minimum" dwell time for an element results in a reduction of precision, whereas collection of data above this "minimum" dwell time should increase precision. For studies incorporating hundreds or thousands of analyses, an optimum dwell time becomes a highly important factor for both a timely and cost effective procedure in which analytical precision is not compromised. Precise results are indicated by a low RSD. Morris (2009) using a pXRF in soil mode on reference materials determined low RSD (< 5%) for Zr, Sr, Mn, Ti, Fe, and Ca and higher RSD for Cu (18%) and Ba (24%).

Till-1, NIST 610, DLH 7, and DLH 10b were analysed using variable dwell times (Appendix A, Appendix C; Fig. 7-14; Tables 4, 5, 6, and 7). For Till-1, concentrations (and their ± 2σ) for 13 different elements for dwell times of 10, 30, and 60 seconds per filter are plotted in Appendix C. Analyses were carried out on NIST 610, DLH 7, and DLH 10b with dwell times ranging from 5 to 80 seconds (Tables 4 to 7). The mean of the analyses and their respective ± 2σ are plotted in Appendix C to display the effect of dwell time on precision.

Zr data are plotted using 10, 30, and 60 second dwell times on Till-1 (Fig. 7). In all three cases, the mean concentration is about 40 ppm above the recommended value of 502 ppm and illustrates that the accuracy is not dependant on dwell time. However, the RSD of Zr in Till-1 improves from 1.8% for a 10 second dwell time to 1.0% for a 30 second dwell time, but then RSD slightly decreases to 1.3% for a 60 second dwell time. Note however, that uncertainty (± 2σ) changes from 19 ppm, to 9 ppm, to 6.1 ppm with dwell times of 10, 30 and 60 seconds, respectively. For elements examined in this study, Zn is the most sensitive to a change in dwell time (Fig. 8). For dwell times of 10, 30, and 60 seconds, the RSD drops from 11%, to 6.8% to 4.1%, respectively. Again, uncertainty (± 2σ) decreases from 24 ppm, to 11 ppm, to 7.6 ppm with dwell times of 10, 30 and 60 seconds, respectively. However, for most elements (e.g. Zr) precision is scarcely improved by increasing dwell time beyond 30 seconds; thus, when considering efficiency with precision, 30 to 40 seconds may be considered as an optimal dwell time.

The discrimination of sample versus background signal depends, in part, on analytical dwell times. For example, only 3 out of 100 analyses for Cu in Till-1 with a dwell time of 5 seconds (see Appendix A) produced values greater than the Limits of Detection (LOD). Increasing the dwell time to 10 seconds resulted in 77 Cu determinations over the first 100 analyses, i.e. 33 analyses were below the LOD. For these 77 analyses, the mean is 65 ppm with an 18% RSD (Fig. 9); the recommended value for Cu in Till-1 is 47 ppm (Table 1; Fig. 9). The mean concentration for a 30 second dwell time is 56 ppm (15% RSD), and is thus closer to the recommended value. Increasing the dwell time to 60 seconds resulted in a 57 ppm mean concentration and a 9.9% RSD (Fig. 9). The inverse correlation between increased dwell time and reduced RSD in the Till-1 Cu data demonstrate that, at concentrations where the LOD is an issue, increasing dwell time improves accuracy and precision.

For any element present at low concentration levels, increasing the dwell time results in a greater number of counts and should improve analytical precision. Pb concentration values determined at various dwell times for sample DLH 10b are illustrated in Figure 10 and listed in Table 10. Note that DLH 10b has a much lower concentration level (25 ppm) as compared to NIST 610 (426 ppm). All measurements for a dwell time of 5 seconds were below the limits of detection (LOD). Measurements at all other dwell times range from 19 to 24 ppm where the recommended value is 25 ppm. The RSD (Table 10) slightly increases from 10 to 20 seconds, but then drops with increasing dwell time (e.g., 18% at 20 seconds to 8.4% at 80 seconds). The mean uncertainty of ± 2σ shows large decreases from 5-30 seconds, but shows only minor improvement for dwell times beyond that.

Pb values determined at various dwell times for DLH 7 (Fig. 11) display an increase in precision with increasing dwell time, and a fluctuation in accuracy with dwell times from 60-80 seconds (Table 11). Although not plotted on Figure 11, 72 of 112 analyses with dwell times at 5 seconds returned measurements greater than the LOD. Several elements including As, Cr, Fe, K, Mo, Se, and Th display a similar pattern to that displayed by Pb in Figure 11, namely decreasing mean measurements for dwell times of 50, 60, and 70 seconds, and an increase at 80 seconds (Appendix C). Although not as pronounced, other elements such as Cu, Sc, Sr, U, V, and Zr (Table 12, Fig. 12) display an inverse pattern (as compared to e.g., Pb) with increasing concentrations for dwell times of 50, 60, and 70 seconds and a decrease in concentration for a dwell time of 80 seconds (Appendix C). Note that all mean concentration levels for Zr are ~20% higher than the recommended value of 68 ppm.

| Reference material | Dwell time / filter (s) | Number of analyses | Pb mean concentration (ppm) | Pb mean error ±2σ (ppm) | %RSD |
|---|---|---|---|---|---|
| DLH 10b | 5 | 116 | <LOD | | |
| DLH 10b | 10 | 72 | 23.8 | 15 | 18 |
| DLH 10b | 20 | 114 | 19.8 | 7.5 | 19 |
| DLH 10b | 30 | 116 | 20.1 | 5.8 | 14 |
| DLH 10b | 40 | 162 | 20.1 | 4.9 | 12 |
| DLH 10b | 50 | 113 | 19.7 | 4.3 | 11 |
| DLH 10b | 60 | 115 | 19.5 | 3.9 | 9.9 |
| DLH 10b | 70 | 111 | 19.3 | 3.6 | 9.4 |
| DLH 10b | 80 | 105 | 19.9 | 3.4 | 8.4 |

Table 10. Variable dwell times with mean Pb concentration, mean error of ±2σ and %RSD from Appendix A for DLH 10b. Recommended Pb concentration for DLH 10b is 85 ppm.

| Reference material | Dwell time / filter (s) | Number of analyses | Pb mean concentration (ppm) | Pb mean error ±2σ (ppm) | %RSD |
|---|---|---|---|---|---|
| DLH 7 | 5 | 72 | 67.4 | 40 | 19 |
| DLH 7 | 10 | 116 | 53.7 | 14 | 13 |
| DLH 7 | 20 | 110 | 54.3 | 8.3 | 8.1 |
| DLH 7 | 30 | 112 | 53.7 | 6.5 | 5.9 |
| DLH 7 | 40 | 115 | 52.7 | 5.5 | 5.6 |
| DLH 7 | 50 | 115 | 44.5 | 4.5 | 20 |
| DLH 7 | 60 | 148 | 41.3 | 3.1 | 19 |
| DLH 7 | 70 | 104 | 37.8 | 3.6 | 11 |
| DLH 7 | 80 | 105 | 48.9 | 3.6 | 19 |

Table 11. Variable dwell times with mean Pb concentration, mean error of ±2σ and %RSD from Appendix A for 7. Recommended Pb concentration for DLH 7 is 64 ppm.

| Reference material | Dwell time / filter (s) | Number of analyses | Zr mean concentration (ppm) | Zr mean error ±2σ (ppm) | %RSD |
|---|---|---|---|---|---|
| DLH 7 | 5 | 112 | 83.4 | 20 | 11 |
| DLH 7 | 10 | 116 | 81.5 | 7.9 | 5.1 |
| DLH 7 | 20 | 110 | 81.2 | 4.8 | 3.1 |
| DLH 7 | 30 | 112 | 81.4 | 3.7 | 2.5 |
| DLH 7 | 40 | 115 | 80.8 | 3.2 | 1.9 |
| DLH 7 | 50 | 115 | 82.3 | 2.8 | 2.5 |
| DLH 7 | 60 | 148 | 83.6 | 1.9 | 1.5 |
| DLH 7 | 70 | 104 | 84.1 | 2.3 | 1.6 |
| DLH 7 | 80 | 105 | 82.6 | 2.2 | 1.9 |

Table 12. Variable dwell times with mean Zr concentration, mean error of ±2σ and %RSD from Appendix A for DLH 7. Recommended Zr concentration for DLH 7 is 72 ppm.

| Reference material | Dwell time / filter (s) | Number of analyses | Ca mean concentration (ppm) | Ca mean error ±2σ (ppm) | %RSD |
|---|---|---|---|---|---|
| NIST 610 | 5 | 171 | 82608 | 2721 | 1.6 |
| NIST 610 | 10 | 115 | 83029 | 813 | 0.7 |
| NIST 610 | 20 | 116 | 83575 | 486 | 0.5 |
| NIST 610 | 30 | 112 | 83725 | 379 | 0.5 |
| NIST 610 | 40 | 104 | 84046 | 322 | 0.4 |
| NIST 610 | 50 | 176 | 82843 | 281 | 9.2 |
| NIST 610 | 60 | 125 | 83951 | 257 | 0.5 |
| NIST 610 | 70 | 105 | 83917 | 237 | 0.5 |
| NIST 610 | 80 | 117 | 72438 | 196 | 30 |

Table 13. Variable dwell times with mean Ca concentration, mean error of ±2σ and %RSD from Appendix A for NIST 610. Certified Ca concentration for NIST 610 is 81500 ppm.

| Reference material | Dwell time / filter (s) | Number of analyses | As mean concentration (ppm) | As mean error ±2σ (ppm) | %RSD |
|---|---|---|---|---|---|
| NIST 610 | 5 | 171 | 384 | 88 | 11 |
| NIST 610 | 10 | 115 | 388 | 37 | 4.7 |
| NIST 610 | 20 | 116 | 386 | 22 | 3.0 |
| NIST 610 | 30 | 112 | 386 | 17 | 2.4 |
| NIST 610 | 40 | 104 | 388 | 15 | 2.1 |
| NIST 610 | 50 | 176 | 386 | 13 | 2.6 |
| NIST 610 | 60 | 125 | 387 | 12 | 1.8 |
| NIST 610 | 70 | 105 | 385 | 11 | 1.5 |
| NIST 610 | 80 | 117 | 376 | 11 | 5.7 |

Table 14. Variable dwell times with mean As concentration, mean error of ±2σ and %RSD from Appendix A for NIST 610. Recommended As concentration for is 340 ppm.

| Reference material | Dwell time / filter (s) | Number of analyses | Pb mean concentration (ppm) | Pb mean error ±2σ (ppm) | %RSD |
|---|---|---|---|---|---|
| NIST 610 | 5 | 171 | 432 | 99 | 12 |
| NIST 610 | 10 | 115 | 429 | 41 | 4.9 |
| NIST 610 | 20 | 116 | 425 | 25 | 3.3 |
| NIST 610 | 30 | 112 | 424 | 19 | 2.6 |
| NIST 610 | 40 | 104 | 426 | 16 | 2.1 |
| NIST 610 | 50 | 176 | 424 | 15 | 2.5 |
| NIST 610 | 60 | 125 | 428 | 13 | 2.3 |
| NIST 610 | 70 | 105 | 426 | 12 | 1.7 |
| NIST 610 | 80 | 117 | 417 | 12 | 4.4 |

Table 15. Variable dwell times with mean Pb concentration, mean error of ±2σ and %RSD from Appendix A for NIST 610. Certified Pb concentration for NIST 610 is 426 ppm.

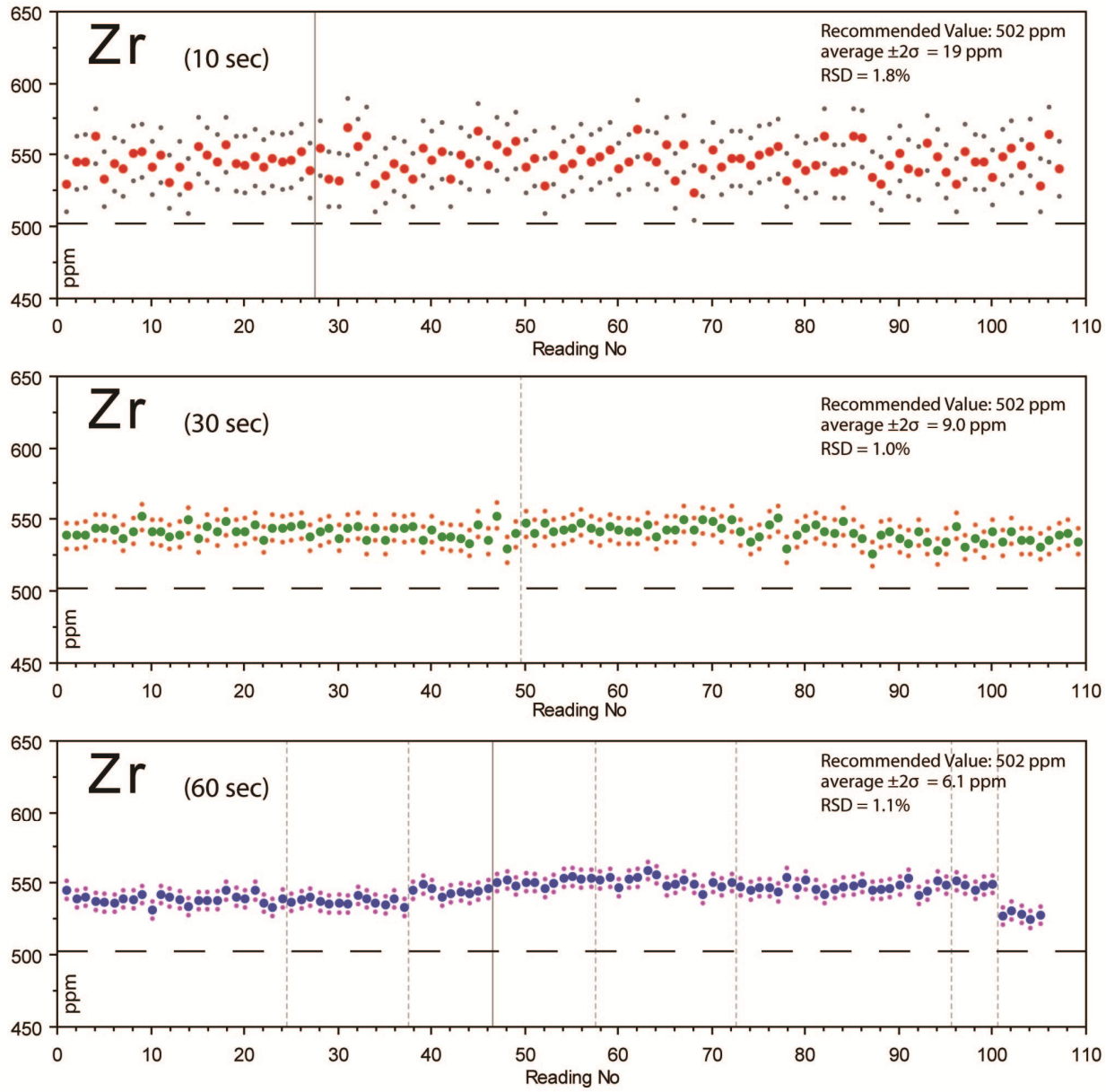


Figure 7. Analyses of Zr in Till-1 with a dwell time of 10, 30, and 60 seconds per filter. Dashed horizontal line represents the recommended value. Dashed vertical lines represent time gaps in analyses when the pXRF was shut down. Solid vertical lines represent a break in analyses from one day to a separate day. Large dots represent the data point with small dots representing ±2σ.

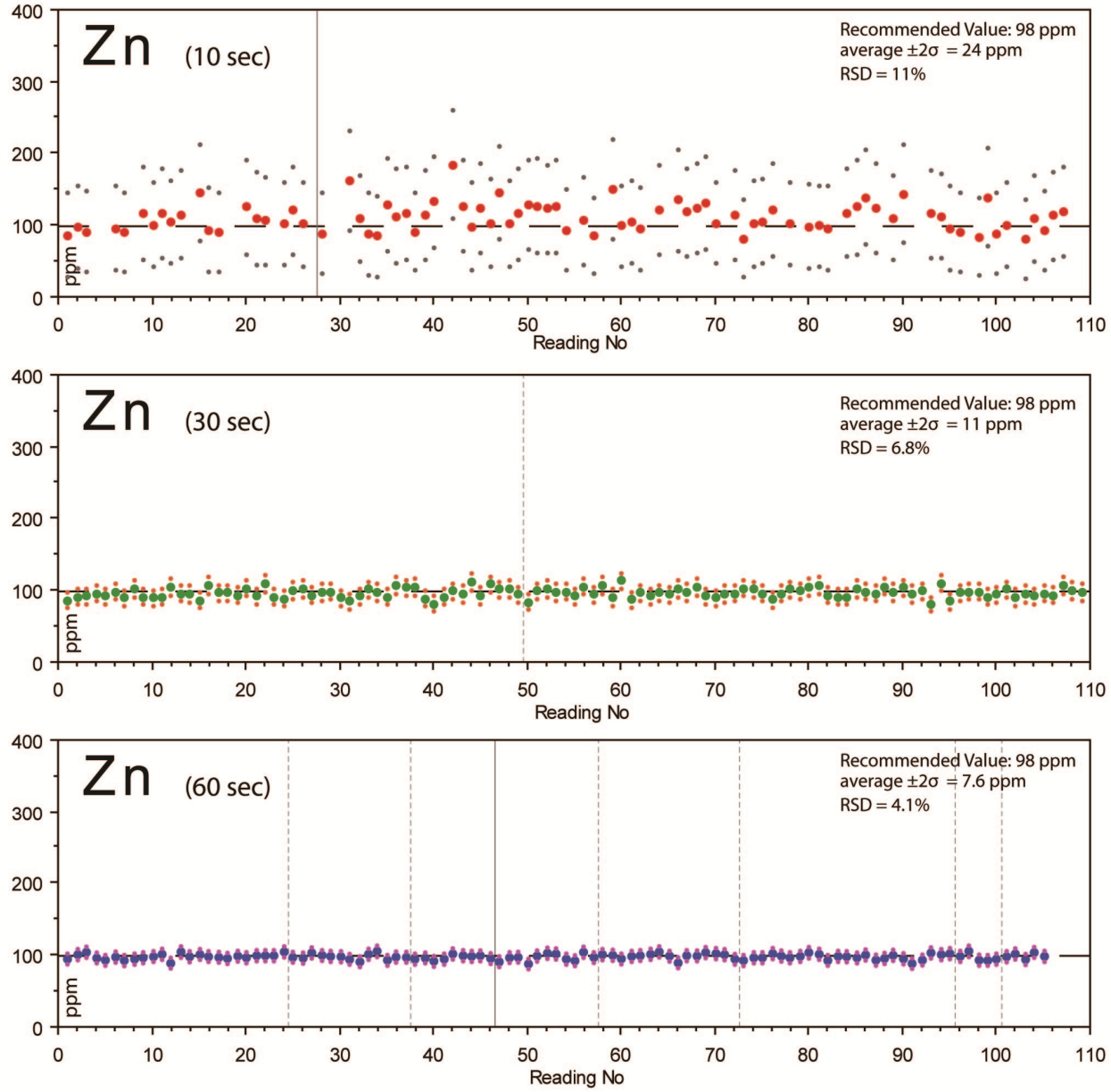


Figure 8. Analyses of Zn in Till-1 using 10 second, 30 second, and 60 second dwell times per filter. Dashed horizontal line represents the recommended value. Dashed vertical lines represent time gaps in analyses when the pXRF was shut down. Solid vertical lines represent a break in analyses from one day to a separate day. Large dots represent the data point with small dots representing ±2σ.

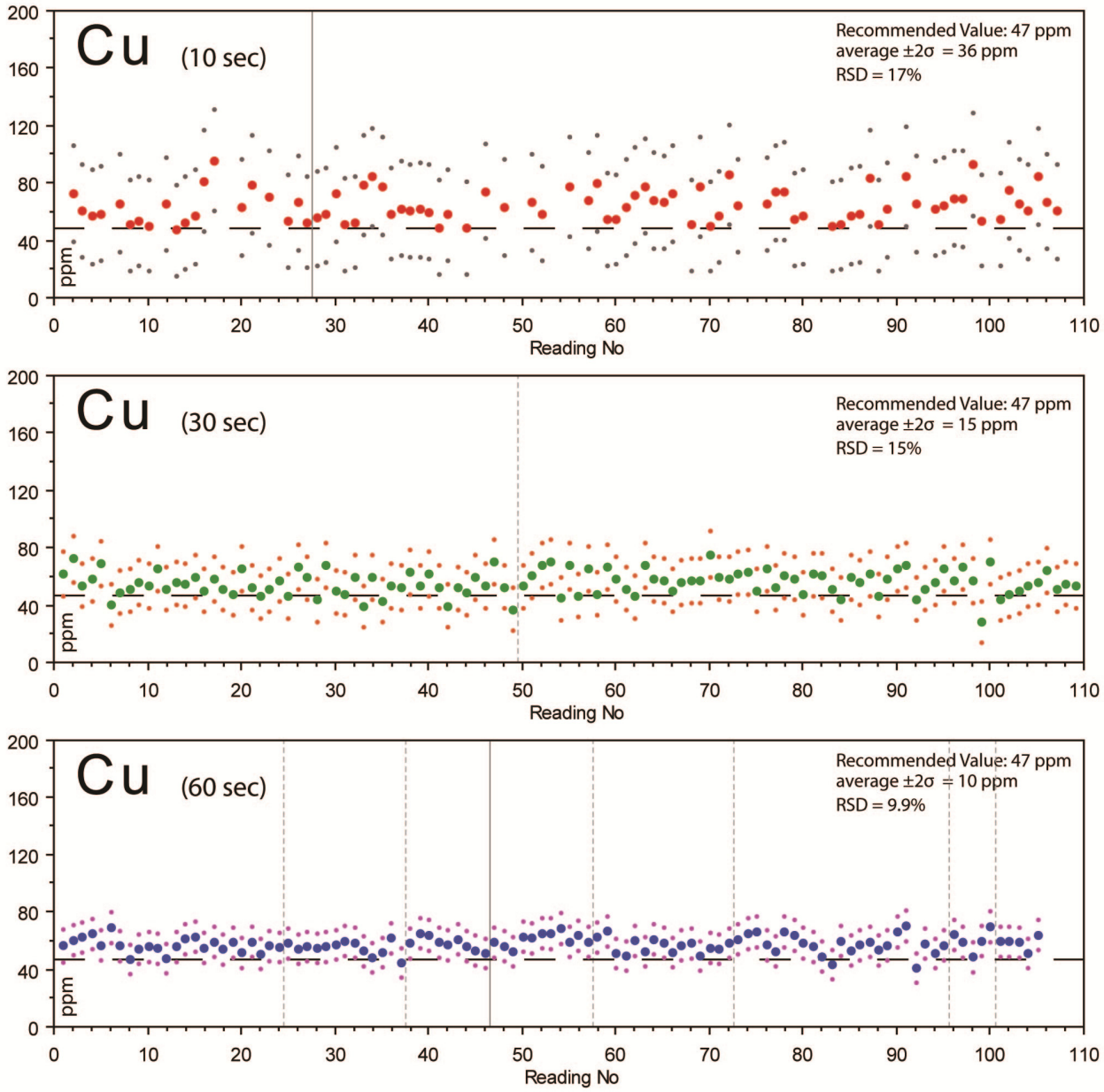


Figure 9. Analyses of Cu in Till-1 with a dwell time of 10, 30, and 60 seconds per filter. Dashed horizontal line represents the recommended value. Dashed vertical lines represent time gaps in analyses when the pXRF was shut down. Solid vertical lines represent a break in analyses from one day to a separate day. Large dots represent the data point with small dots representing ±2σ.

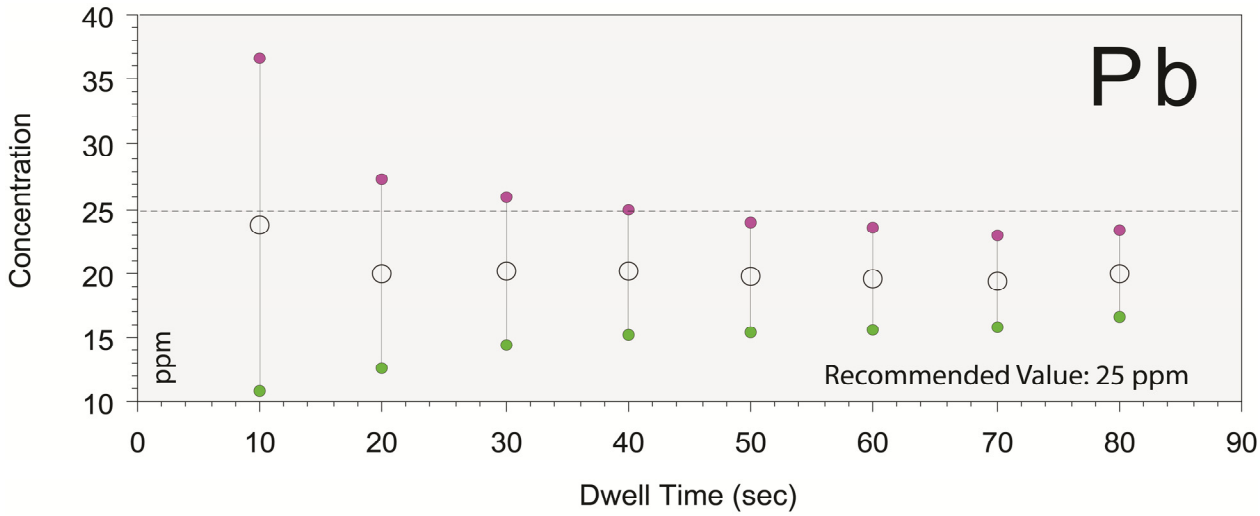


Figure 10. Variable dwell times with mean Pb concentration and mean error of ±2σ as determined by pXRF spectrometry for DLH 10b.

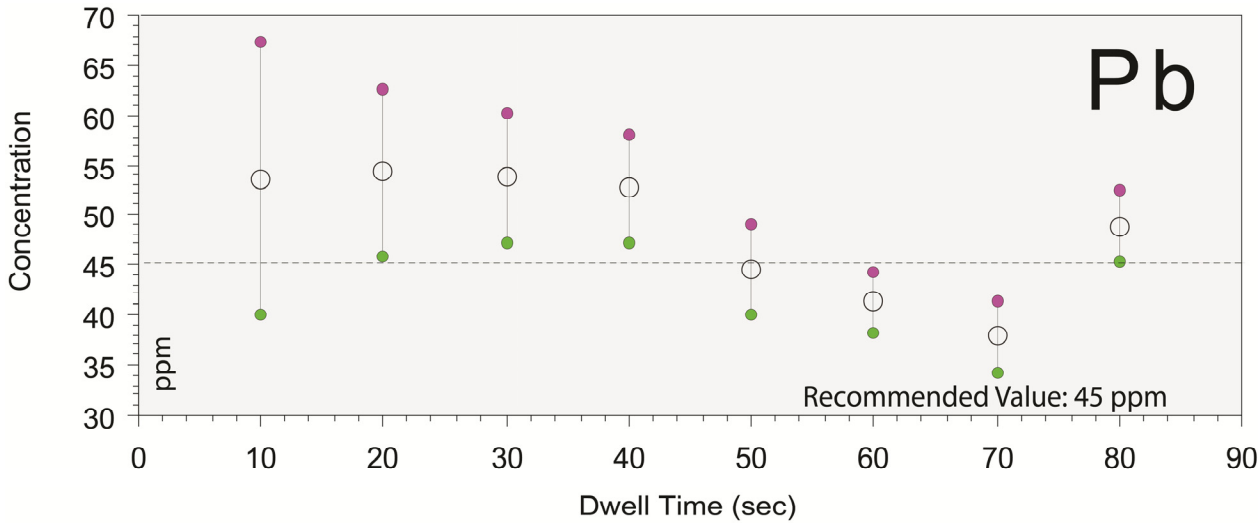


Figure 11. Variable dwell times with mean Pb concentration and mean error of ±2σ as determined by pXRF spectrometry for DLH 7.

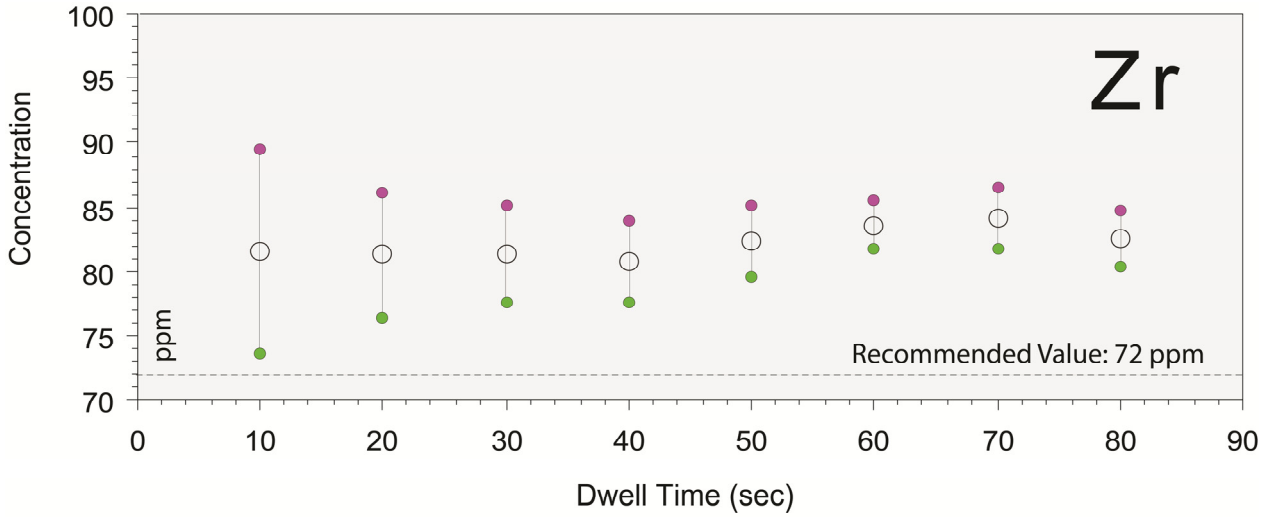


Figure 12. Variable dwell times with mean Zr concentration and mean error of ±2σ as determined by pXRF spectrometry for DLH 7.

### 3.1 Possible effects of detector saturation

Mean concentration measurements and associated error (± 2σ) for dwell times from 5 to 80 seconds for Ca in NIST 610 are listed in Table 13 and illustrated in Figure 13 (see also Appendix A). For all dwell times, pXRF mean Ca concentrations are ~2-3% higher than the certified reference value of 81500 ppm. For these analyses, the pXRF was in soil mode using Compton normalization, which is optimized for samples where elements-of-interest have concentrations <1% (10000 ppm). However, the NIST 610 sample has element concentrations that are over 8%, which may account for some of the variability in the analysed concentration levels. The precision for Ca improves with increasing dwell times of 5 through 40 seconds (Table 13) until a dwell time of 50 seconds at which point the RSD increases from 0.4% at 40 seconds to 9.2% at 50 seconds. This is due to 4 individual analyses with measurements of ~33000 ppm that contribute to a reduced mean concentration. These results are italicized in Appendix A. With dwell times of 60 and 70 seconds there are no anomalous results and no increase in precision (RSD of 0.5%, similar to 20, 30, 40 second dwell times). However, at a dwell time of 80 seconds the first 27 analyses return values just above 33000 ppm, similar to the 4 anomalous results obtained at a dwell time of 50 seconds. At a dwell time of 80 seconds the mean Ca measurement decreases to 72438 ppm, a value lower than any previous dwell time and far lower than the certified value of 81500 ppm. We suggest that these anomalous results may be caused by detector saturation, possibly due to high count rates and increased dead time (Goldstein et al., 1992); however, this is difficult to determine since there is a lack of information regarding the beam current or count-rates at the detector.

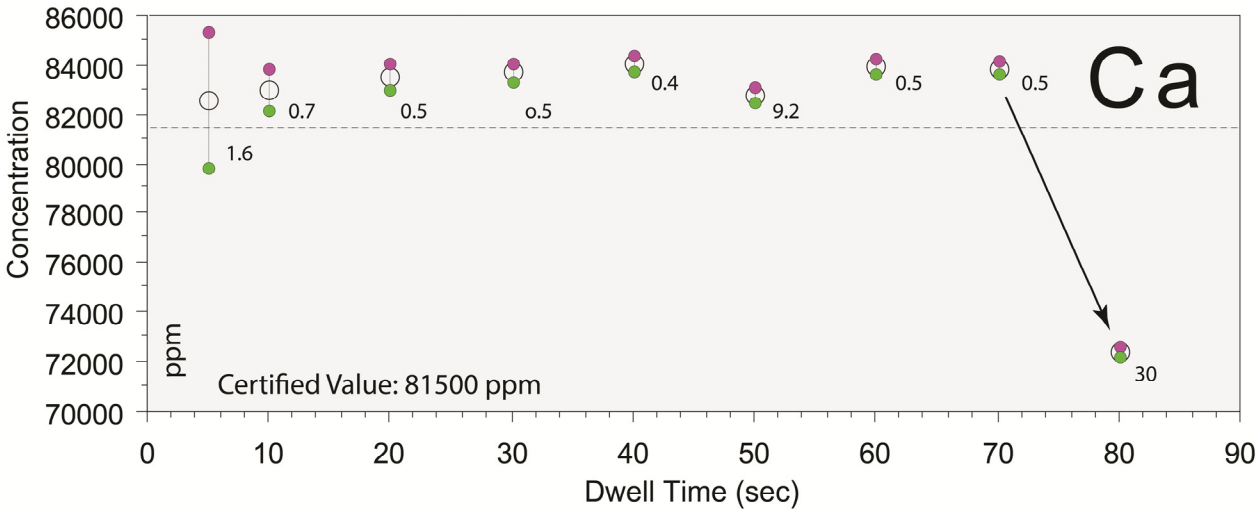


Figure 13. Variable dwell times with mean Ca concentration, mean error of ±2σ (red and green dots), and the %RSD value (number) as determined by pXRF spectrometry for NIST 610.

### 3.2 Summary of dwell time effects

In general, accuracy is not affected by dwell time, whereas precision improves with dwell time. We have demonstrated that precision is usually only slightly improved for dwell times beyond 30 to 40 seconds (for many, but not all elements). As a result, we suggest that for many studies the optimal analytical time frames should be >30 seconds to 60 seconds and not exceeding 70 seconds. Exceptions to these trends were seen with very low (i.e., close to LOD) or very high concentrations. When concentrations are close to the LOD, longer dwell times improve accuracy in addition to precision. For very high concentrations, shorter dwell times are appropriate in order to avoid potential detector saturation that may cause inaccurate results. Increasing the dwell time increases the precision (decreases ± 2σ) however, after 40 seconds of dwell time there is little reduction in ± 2σ (Fig. 11 to 13).

## 4.0 Element interference

Two examples of element interference provide some insight into the importance of choosing a pXRF spectrometer that assures that the collected data is aligned with project goals. A major criticism of pXRF spectrometry is its inability to differentiate key elements in some geological problems of interest. For example, it is well understood that the resolution of Ba and Ti can be difficult due to the Ba Lα (4.47 keV) and Ba Lß (4.83 keV) overlap with the Ti $K\alpha_1$ (4.51 keV) spectral peak. The Niton pXRF spectrometer with a Cygnet 50 kV X-ray tube utilizes the Ba $K\alpha_1$ (32.19 keV) peak in the high energy portion of the spectrum that removes the issue of Ti interference on Ba; however, there remains the problem of Ba interference on the Ti $K\alpha_1$ analytical peak.

Mean Ba and Ti concentrations obtained at various dwell times for Till-1 are plotted with the recommended value in Figure 14. The precision and accuracy at dwell times of greater than 30 seconds are considered excellent (RSDs of 3.9% and 1.1%, respectively; means 3.1% above and 0.1% below their respective recommended values). Resolution of Ba and Ti in Till-1, -2, -3, -4 and TCA8010 are also excellent (Appendix B). Knight et al. (2012) analyzed 80 samples of fine-grained sediment collected from a Champlain Sea borehole (using the same pXRF instrument as in this study) and detected Ba with a mean concentration of 284 ppm, which is significantly lower than fusion ICP-ES mean concentration of 839 ppm for the same sample. Mean Ti measurements were 3820 ppm by pXRF and 4320 ppm by fusion ICP-ES. Although the pXRF and fusion ICP-ES results are not identical, the pXRF produces similar down-hole trends for Ba and Ti as compared to the ICP-ES data (Fig. 15).

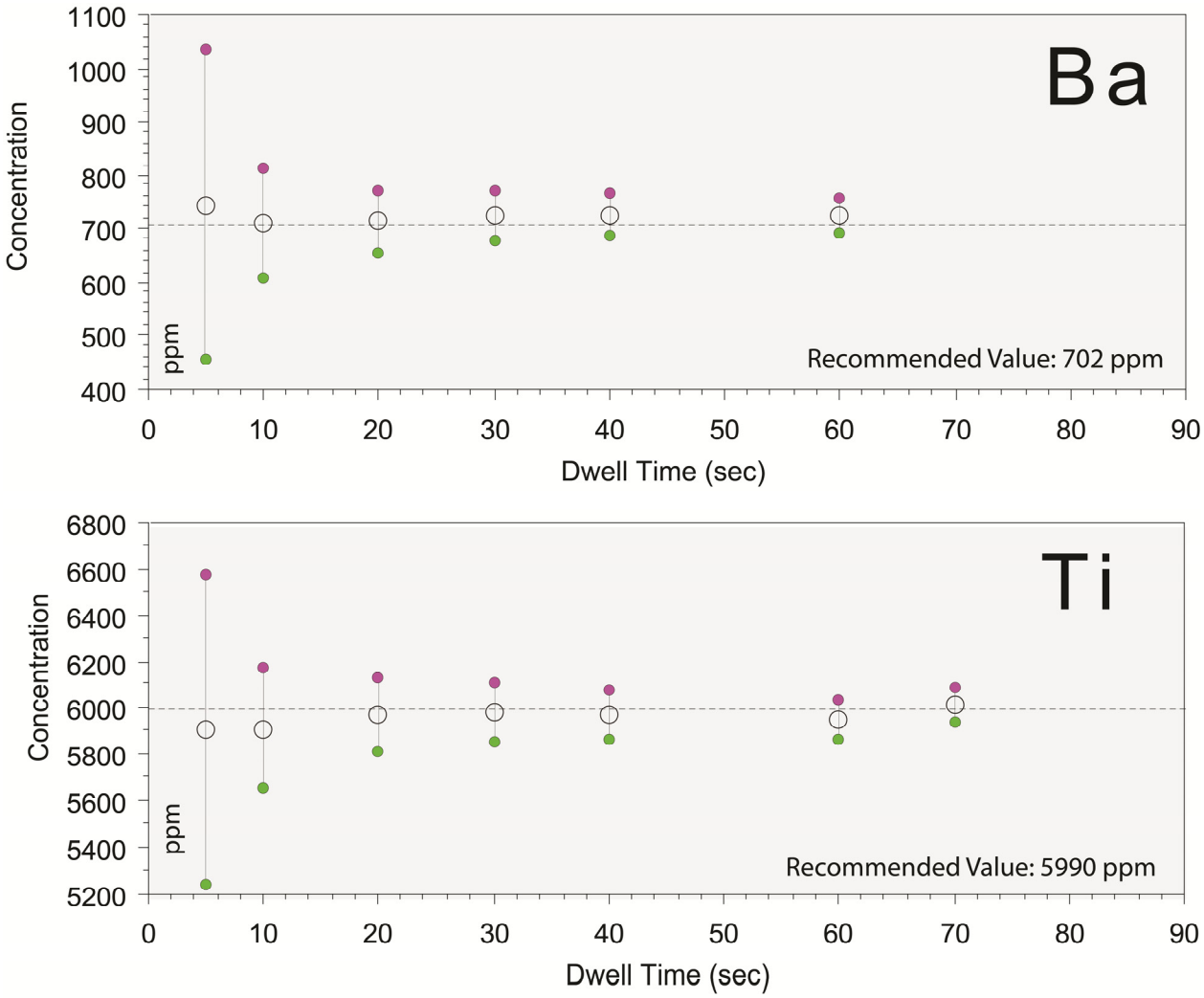


Figure 14. Variable dwell times for mean Ba and Ti concentrations with mean error of ±2σ as determined by pXRF spectrometry for Till-1 with recommended values plotted as horizontal dashed lines.

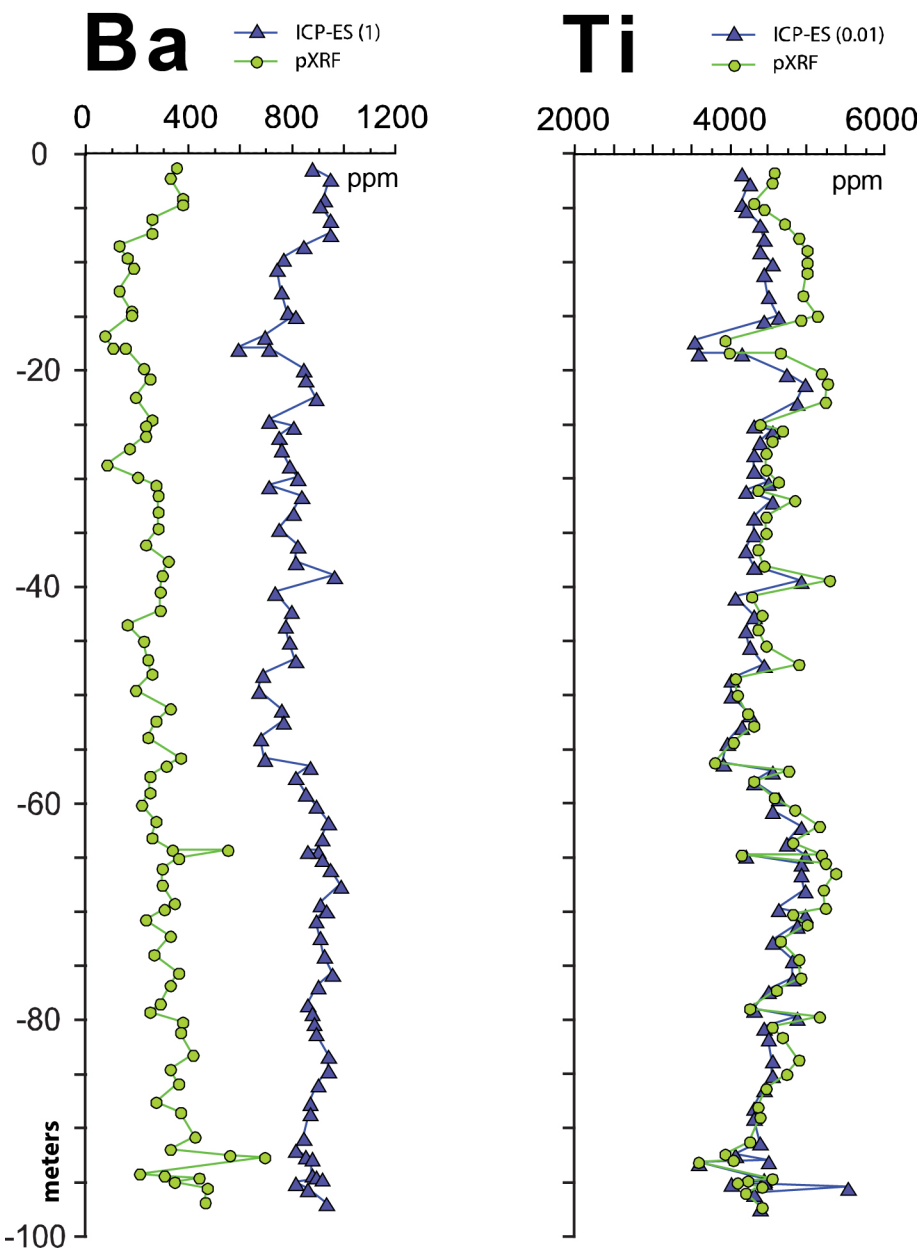


Figure 15. Chemostratigraphy of Ba and Ti by pXRF spectrometry and ICP-ES fusion methods from a borehole in Champlain Sea sediments located near Kinburn Ontario. Modified from Knight et al., 2012. Note that the Ba data from the pXRF has 4 spikes that are not observed in the ICP-ES data.

For DLH 7, utilizing a dwell time of 60 seconds, Ba was detected 4 times out of 148 analyses, with a mean of 36 ppm, compared to the recommended value of 65 (Table 2); the reported detection limit for an $SiO_2$+Fe+Ca matrix material is 45 ppm (Thermo Scientific, 2008) suggesting that the 4 analyses are most likely noise as they are below the detection limit. The recommended Ti value is also below the detection limit of the pXRF spectrometer. One hundred and fifteen analyses of DLH 10b using the pXRF with a dwell time of 60 seconds returned a mean Ba measurement of 69 ppm and a mean Ti measurement of 506 ppm. Both values are well below the recommended concentrations of 900 ppm for Ba and 930 ppm for Ti. For 125 analyses of NIST 610 at dwell time of 60 seconds, the mean Ti measurement was 530 ppm, while the recommended value is 437 ppm. All Ba measurements were below the LOD, despite a recommended value of 453 ppm; we originally thought this was due to matrix effects, as NIST 610 (along with DLH 7 and DLH 10b) is a glass, and not a soil. The Ba $K\alpha_1$ the peak at 32.19 keV is present in the peak profile for NIST 610 (Fig. 16), but the peak is misidentified as iodine (I). Our data suggest that when Ti concentrations are above ~1000 ppm Ba is detected, but when Ti concentrations are below ~1000 ppm Ba is not detected, although this needs to be further tested to be verified.

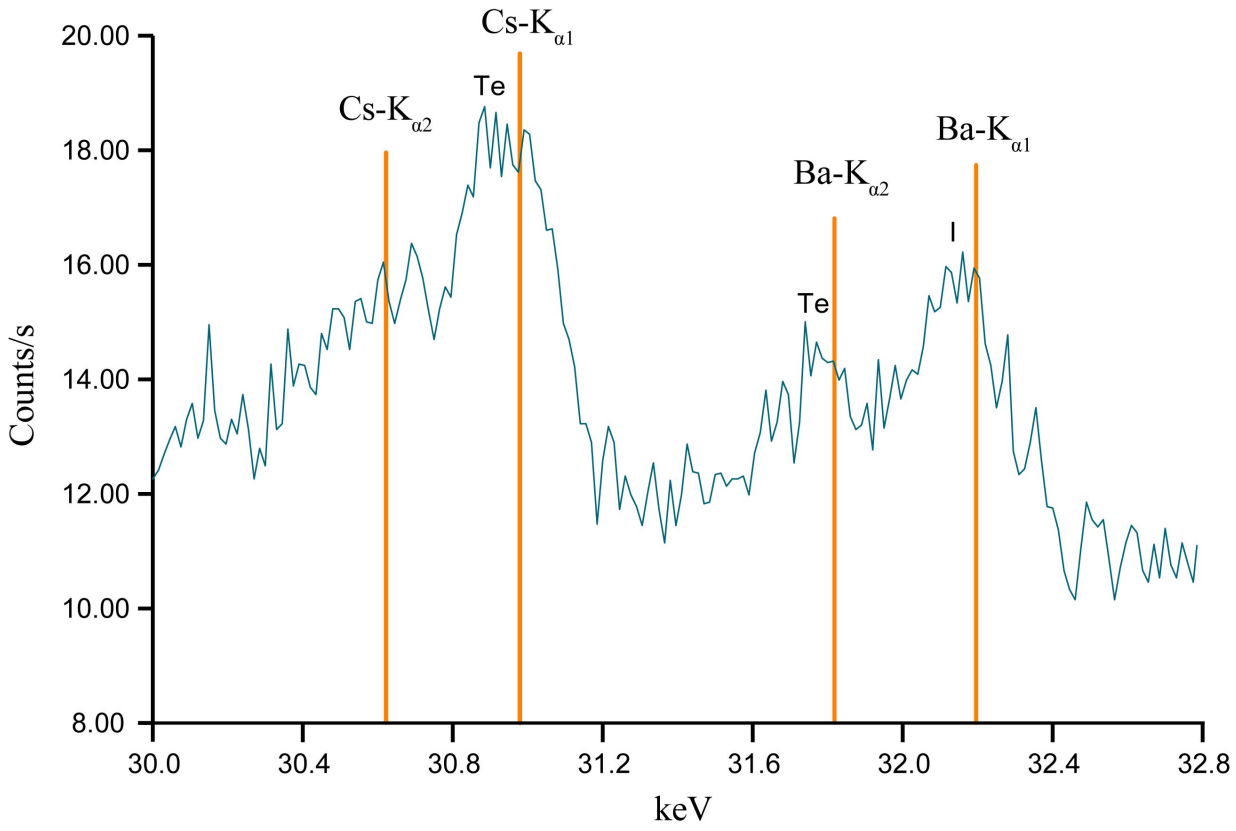


Figure 16. Spectral measurement for NIST 610 at 60 seconds. Peaks for Te and I are labelled by Niton NDT software, while orange lines are accepted emission lines for Ba and Cs.

Peak overlaps are also present for As and Pb, with the As Kα peak at 10.53 keV and the Pb Lα peak at 10.55 keV. Pb is differentiated from As by utilizing the 12.61 keV Lβ peak for Pb (Table 6), however, sensitivity of detection can be affected by use of the Lβ peak since the intensity is only half that of the Lα peak. The Pb Lα peak at 10.55 keV, however, is still an issue for the analysis of As. Stanley et al. (2009) using a NITON XLt 792Y pXRF spectrometer suggests that if Pb concentrations exceed 1%, pXRF spectrometry generates inaccurate and high As results. NIST 2780 contains the highest Pb concentrations analysed during this study (Table 2). Thirty-four analyses were carried out on NIST 2780, recording a mean of 5111 ppm Pb, with 12 analyses returning As measurements above the LOD. These 12 samples had a mean As value of 52 ppm, which is within the analytical uncertainty for the recommended value of 48.8 ppm. The reported detection limit of As in a $SiO_2$+Fe+Ca matrix material is 7 ppm (Thermo Scientific, 2008). The Pb content NIST 2780 is below 1% at ~0.58% and the As measurements in this sample are not elevated from Pb interference. None of the samples analyzed had high-enough Pb concentrations to test Stanley's (2009) hypothesis

As and Pb measurements from NIST 610 at various dwell times are illustrated in Figure 17. The number of analyses, dwell times, mean concentrations, average +/- 2σ, and RSD for As from NIST 610 are listed in Table 14, with data for Pb listed in Table 15. The mean As pXRF measurement for all dwell times is 385 ppm, as compared to a certified concentration level for As of 340 ppm (horizontal dashed line in Fig. 17). The mean Pb pXRF measurement for all dwell times is 425 ppm, statistically the same as the certified concentration value of 426 ppm. NIST 610 is recording precise, but inaccurate As concentrations (mean ~11% too high) that could be corrected with calibration. However, it is recording precise (mean RSD=2.6%) Pb concentrations with dwell times as low as 20 seconds and accurate Pb concentrations for all dwell times.

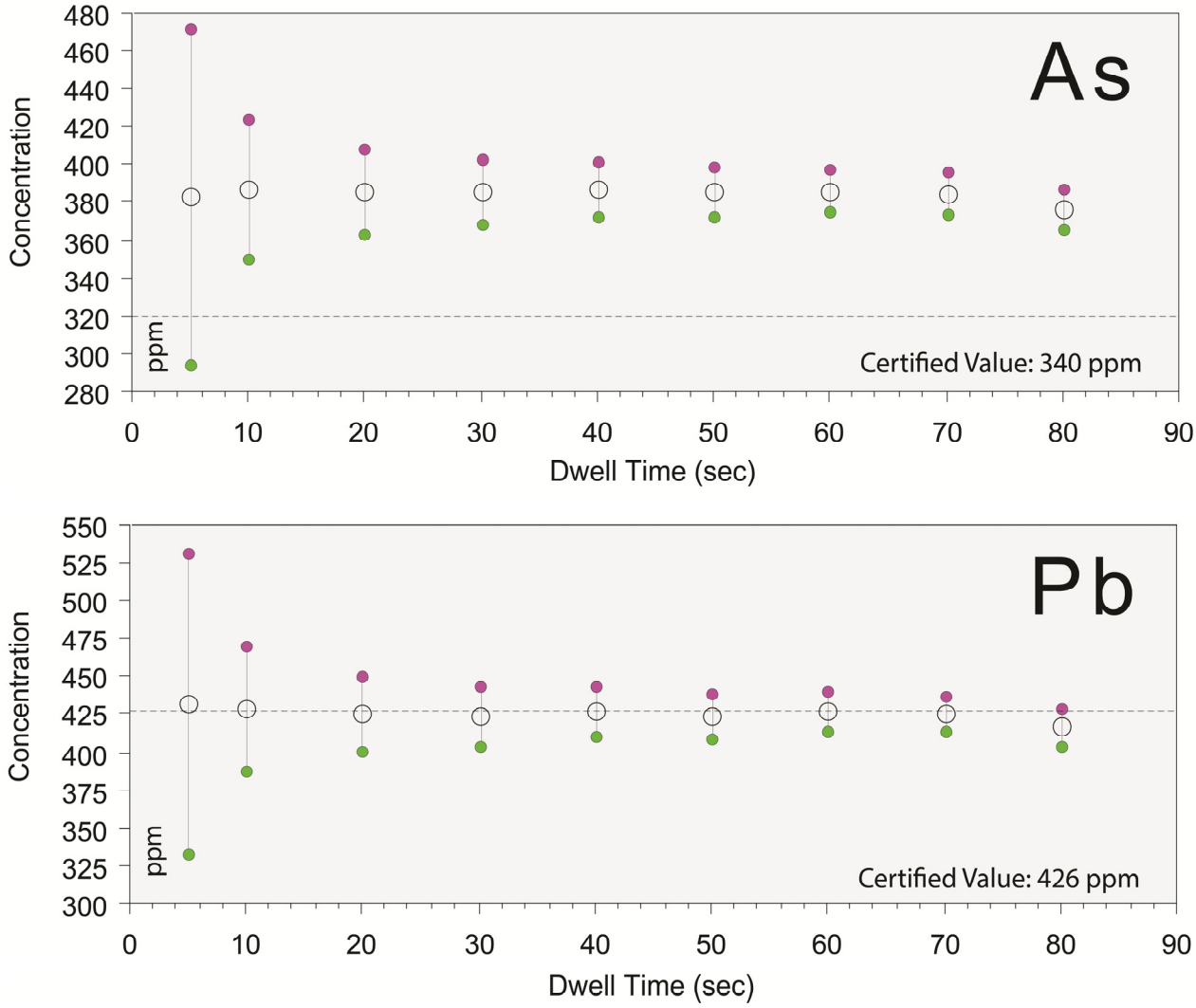


Figure 17. Variable dwell times for mean As and Pb concentrations with mean error of ±2σ as determined by pXRF spectrometry for NIST 610 with recommended values plotted as horizontal dashed lines.

## 5.0 Examining calibrations

Calibration of pXRF spectrometers has been discussed by Weltje and Tjallingii (2008), Radu and Diamond (2009), Kenna et al. (2011), and Rowe et al. (2012). Calibrations are typically carried out: (1) pre-collection, by entering a calibration slope and intercept into the pXRF spectrometer, or; (2) post-collection, by correcting data based on analyses of standard reference materials. The precision and accuracy that can be expected from the Niton pXRF spectrometer over a range of elements and concentrations levels, as determined from 60 s analyses of Till-1, -2, -3, and -4, is

illustrated in Figure 18a and 18b. Ideally, the linear equations expressed in the lower right corner of each graph on Figure 18a and 18b should be valid for all concentrations, but for very high concentrations this may not be the case (i.e. the equations may be limited to concentrations near the analytical range). It should be noted that the Till series of standards is comprised of sediments with a siliciclastic matrix, and thus the equations developed as part of the current study may not apply to sediments with a carbonate or an iron-oxide matrix. In order to test or calibrate a pXRF spectrometer for laboratory or field use, it is necessary to use standards similar to the materials being analysed.

| | Till-1 | Till-2 | Till-3 | Till-4 |
|---|---|---|---|---|
| **As** | 9.0 | 6.6 | 2.8 | 2.6 |
| **Ba** | 2.9 | 3.3 | 3.3 | 4.0 |
| **Ca** | 1.3 | 0.9 | 1.4 | 3.6 |
| **Cr** | 13 | 7.8 | 7.6 | 15 |
| **Cs** | 6.5 | 7.8 | 8.2 | 9.7 |
| **Cu** | 9.9 | 4.0 | 15 | 3.2 |
| **Fe** | 0.6 | 0.5 | 0.7 | 0.8 |
| **K** | 1.3 | 0.8 | 1.0 | 2.5 |
| **Mn** | 2.3 | 3.2 | 5.2 | 4.7 |
| **Ni** | 13 | 14 | 10 | 22 |
| **Pb** | 9.4 | 6.9 | 6.9 | 4.9 |
| **Rb** | 2.3 | 1.4 | 2.2 | 1.6 |
| **Sr** | 0.8 | 1.2 | 0.8 | 1.4 |
| **Th** | 13 | 6.1 | 14 | 3.8 |
| **Ti** | 1.3 | 0.8 | 1.3 | 2.4 |
| **V** | 8.3 | 8.3 | 8.2 | 13 |
| **Zn** | 4.1 | 3.3 | 5.8 | 6.4 |
| **Zr** | 1.4 | 1.1 | 1.8 | 2.5 |

Table 16. Relative standard deviations (%RSD) for all elements consistently recorded in Till 1-4 with a dwell time of 60 seconds.

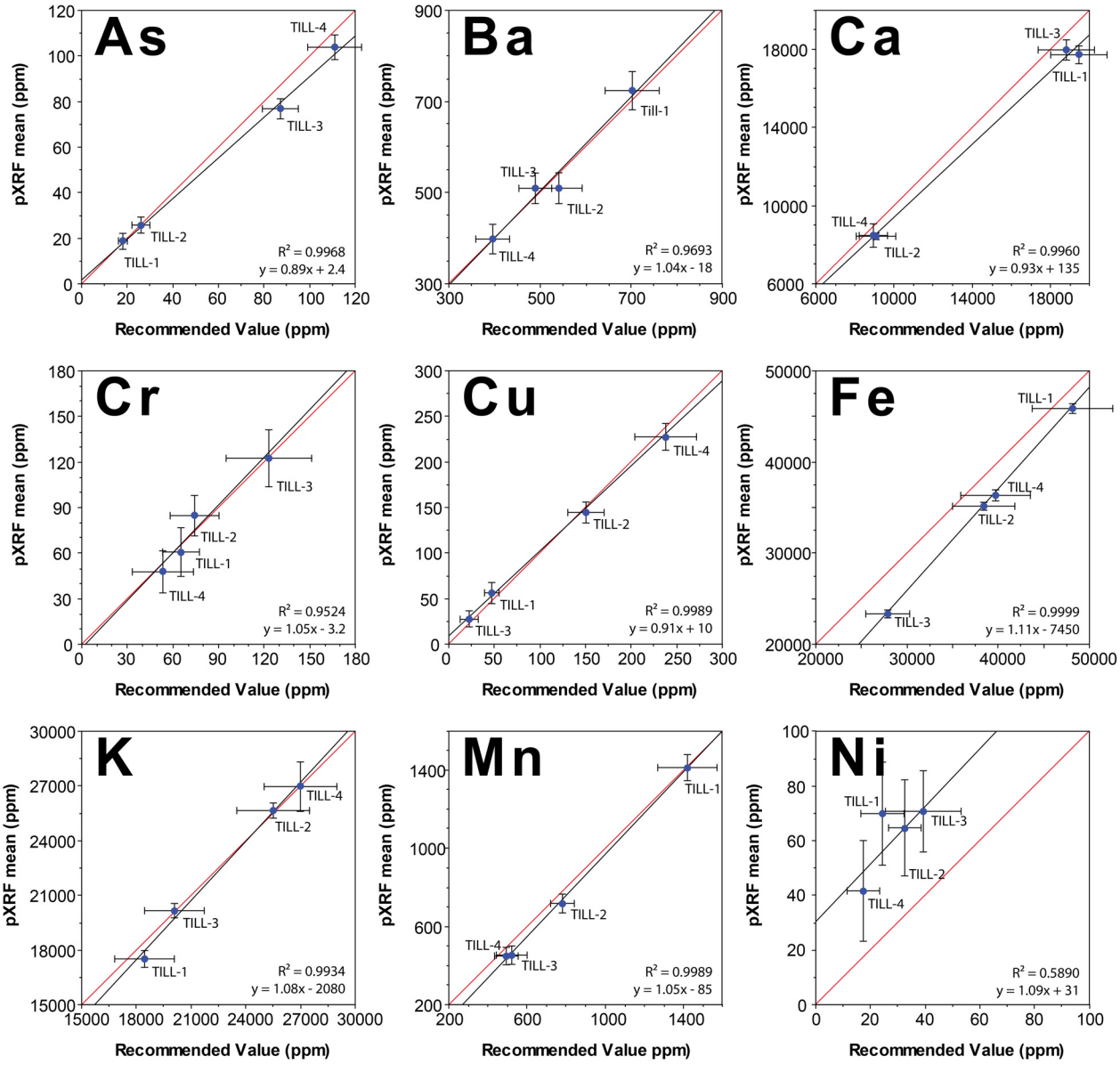


Figure 18a. Recommended value verses mean pXRF data obtained form Till-1, -2, -3, and -4. Horizontal error bars represent two standard deviations of the laboratory analyses, as stated in (Lynch, 1996). Vertical error bars represent two standard deviations of the ~100 pXRF measurements. Red lines represent a 1:1 conversion (y = x).

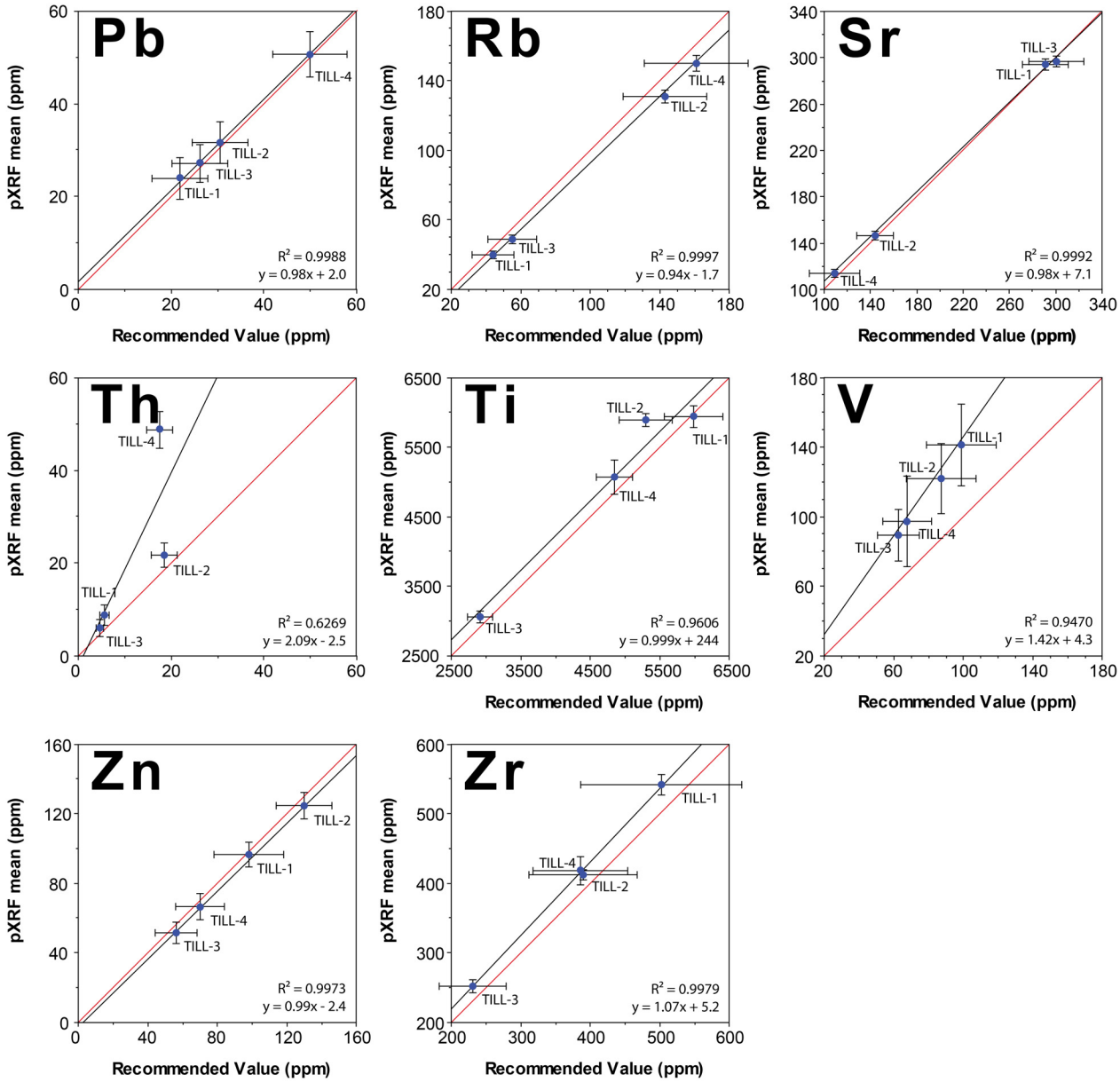


Figure 18b. Recommended value verses mean pXRF data obtained form Till-1, -2, -3, and -4. Horizontal error bars represent two standard deviations of the laboratory analyses, as stated in (Lynch, 1996). Vertical error bars represent two standard deviations of the ~100 pXRF measurements. Red lines represent a 1:1 conversion (y = x).

### 5.1 Factory and post-collection calibrations

For graphs displayed in Figure 18a and 18b the vertical uncertainty bars represent mean ± 2σ of all 60 second measurements, not the ± 2σ associated with the individual measurements provided by the pXRF spectrometer during data acquisition. Table 16 lists the mean ± 2σ for elements detected in Till-1, -2, -3, and -4. For many elements (eg: Ba, Cr, Cu, K, Pb, Sr, and Zn) no calibration is required as the pXRF measurements (mean ± 2σ) falls within the value and error of recommended value. In contrast concentrations of some elements (e.g., Fe) would benefit from post-data collection calibration. For example, Fe has a very high $r^2$ of 0.9999 and was measured precisely (0.6% RSD), but not accurately (m = 1.11; Fig. 17). To calibrate Fe, we utilized a least-squares regression and the correction equation: y = 0.90x + 6730 (where x is the measured concentration and y is the calibrated concentration; Fig. 19). This bivariate plot differs from Figure 17 by reversal of the x and y axes. Results for Fe after post-collection correction for Tills 1 through 4 are displayed in Figure 20.

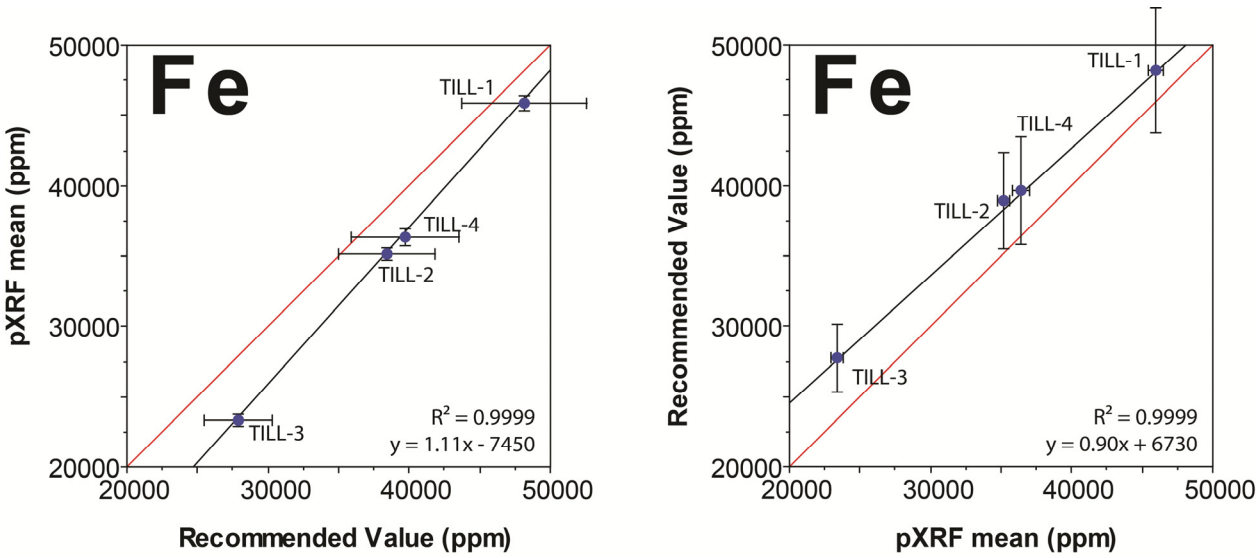


Figure 19. The bivariate plot on the left displays the pXRF mean vs. recommended value for Fe as it is displayed in Figure 18a. For the bivariate plot on the right the axes have been reversed from the plot on the left, and the resulting equation is the calibration factor.

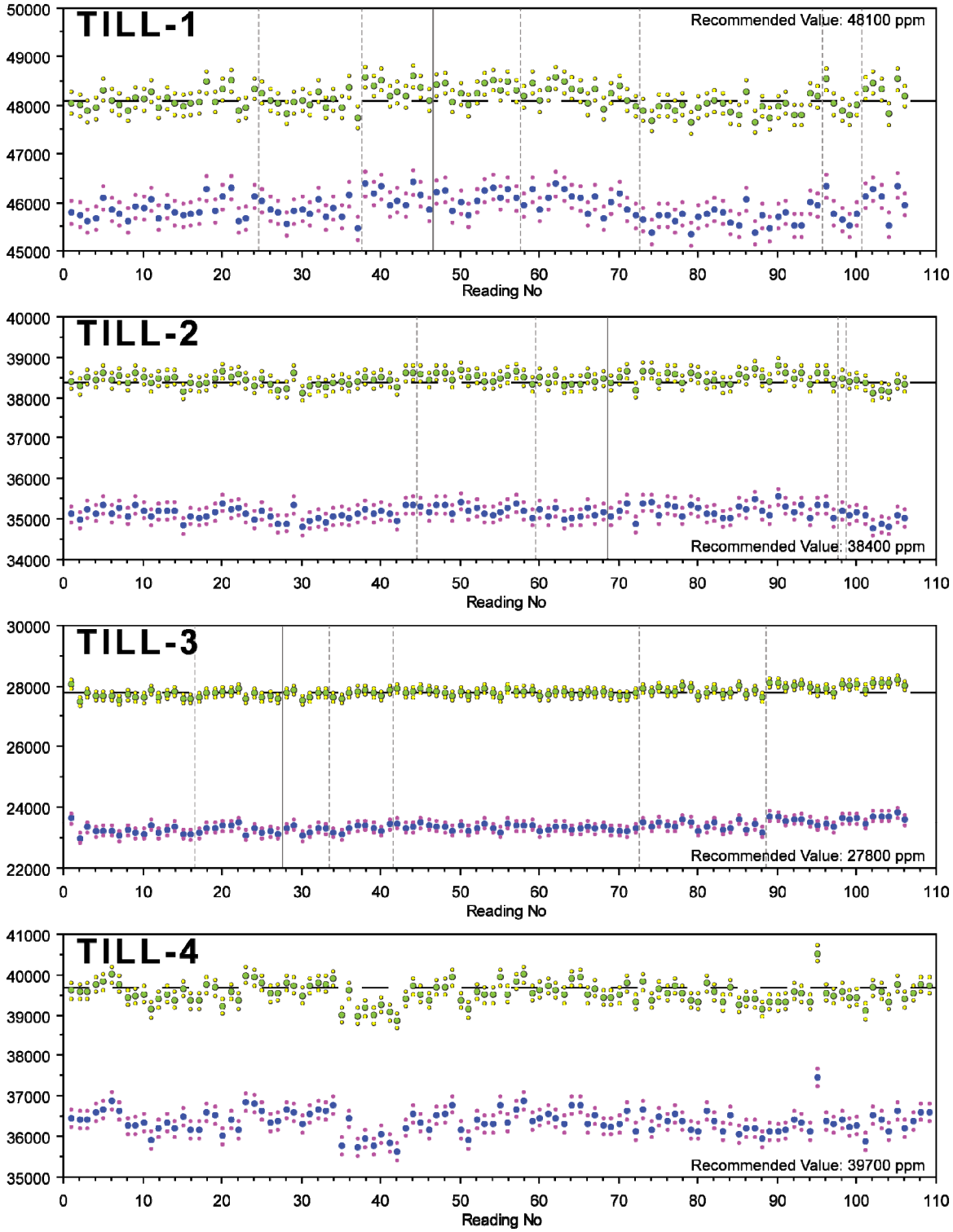


Figure 20. Post-collection data calibration of Fe where original measurements are plotted using blue circles and post collection calibrated data plotted using green circles.

### 5.2 Categorising elements based on results from Till-1, -2, -3, and -4

The eighteen elements detected by pXRF were divided into five categories using the coefficient of determination ($r^2$), %RSD, and slope (m), to represent linearity, precision, and the factory calibration, respectively (Fig. 21). The categories are only valid for Till-1, -2, -3, and -4 and were chosen so that elements which display similar trends are grouped together. However, since these materials are meant to represent a broad range of sediment across Canada, they should provide a practical assessment of the usefulness of pXRF in analysing surficial materials.

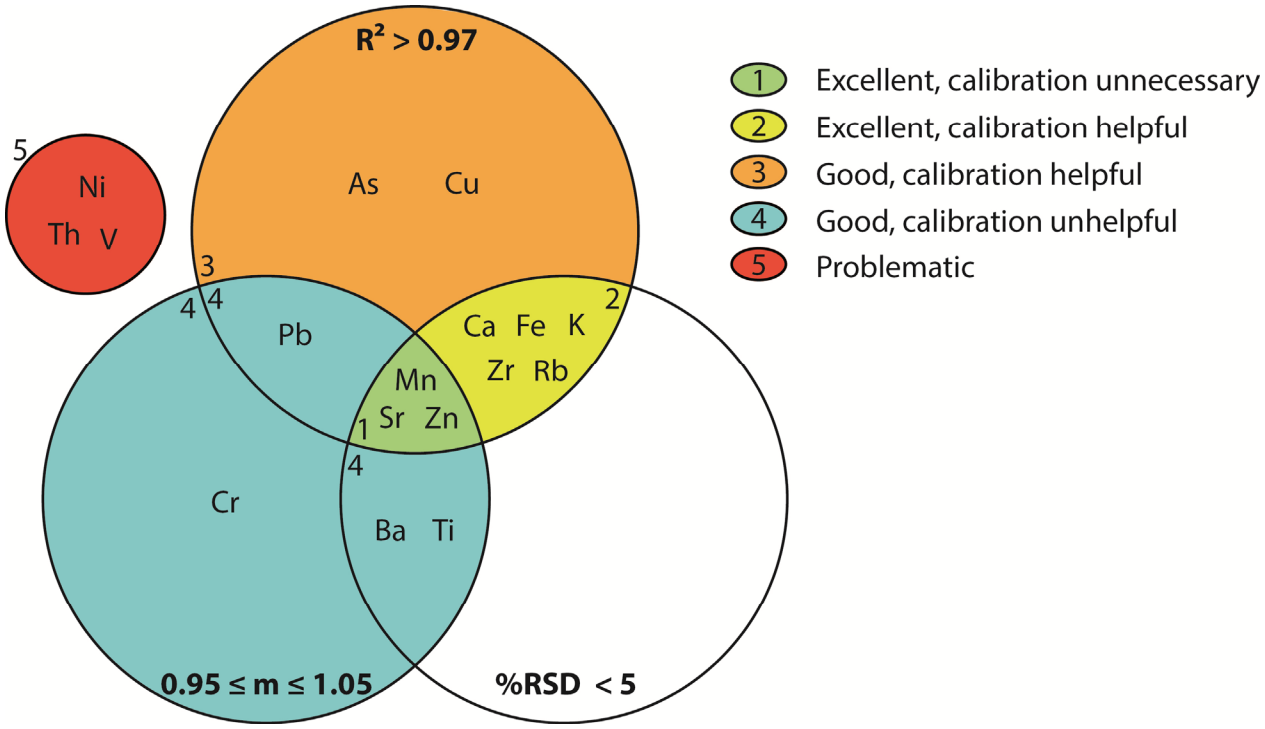


Figure 21. Elements are organized by slope (m), $R^2$, and mean RSD as a means of determining which elements are suitable for calibration.

Elements were categorised using an $r^2$ value of 0.97 that represents a natural break between Ba ($r^2$ = 0.9693) and K ($r^2$ = 0.9934) as illustrated in Figure 22. Slopes with a range of $0.95 \leq m \leq 1.05$ represent the fit of a near-perfect factory calibration (Fig. 23). It is suggested that elements with slopes outside this range would benefit from a post-collection calibration correction. The limits of this range in slope were chosen as they fall in natural breaks between Rb (m = 0.94) and Pb (m = 0.98) on the lower end, and Mn (m = 1.05) and Zr (m = 1.07) on the higher end (Fig. 23). Elements were further categorized based on precision using an arbitrary mean RSD of 5% (Fig 24). RSD is the least reproducible of the three variables as it is the most strongly dependent on the elemental concentrations in the analysed materials. Although an element's ± 2σ uncertainty is

slightly dependent on concentration, it will be proportionally larger for low concentrations. Low concentrations will thus result in higher RSD. However, since Till-1, -2, -3, and -4 cover a large range of concentrations for most elements, the mean RSD is a satisfactory representation of precision.

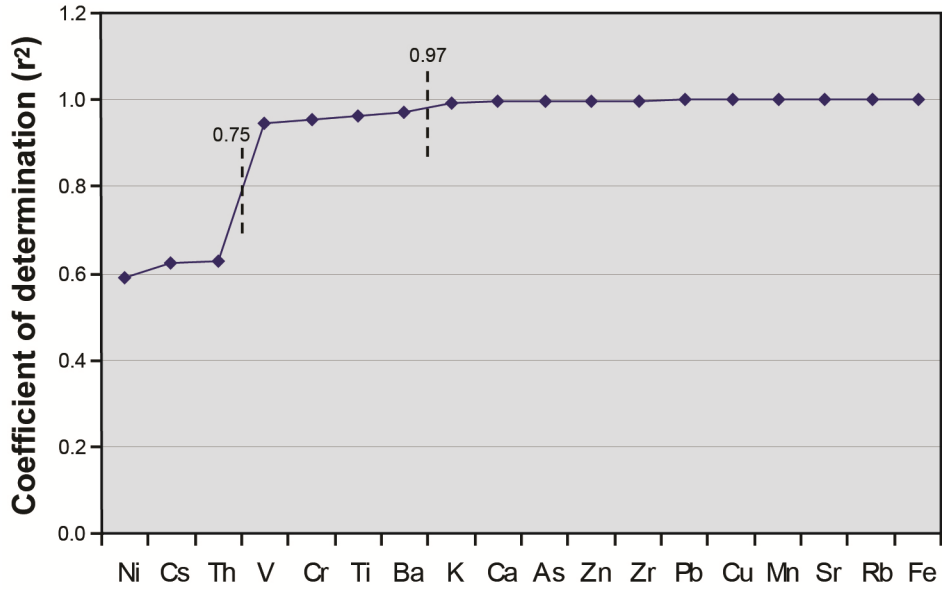


Figure 22. Coefficient of determination ($r^2$) for elements analysed in Till 1-4.

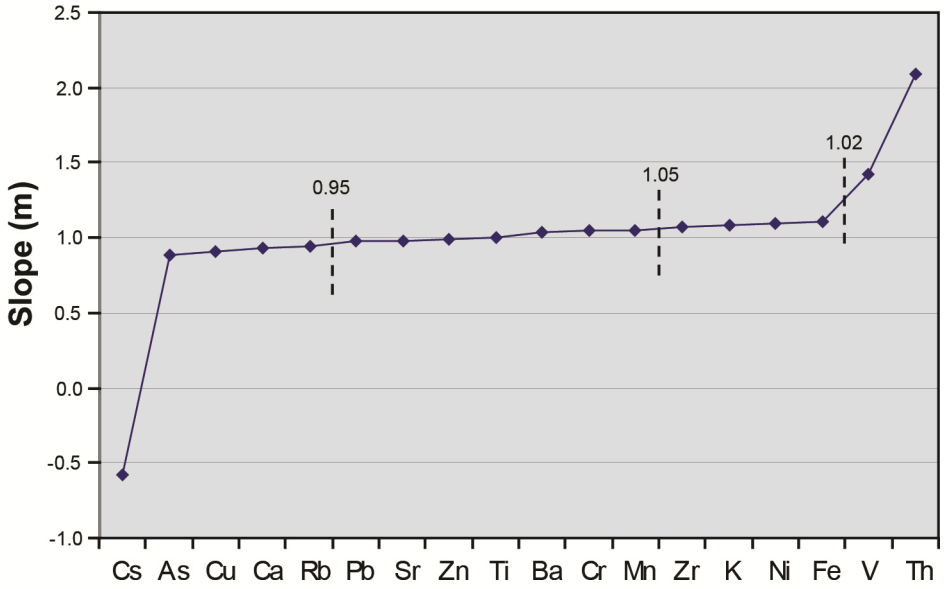


Figure 23. Precision represent by slope (m) for elements analysed in Till 1-4.

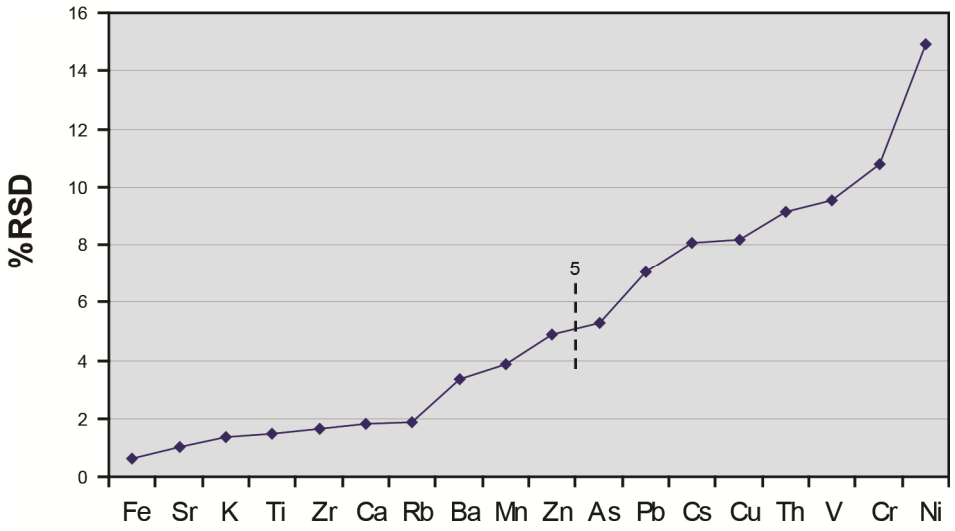


Figure 24. Relative standard deviation (RSD) for elements analysed in Till 1-4.

Elements in categories 1 (Sr, Zn) and 2 (Ca, Fe, K, Mn, Rb, Zr) are both measured with a high degree of precision and linearity (RSD <5%, $R^2$ >0.97), the difference is merely in their calibration; 0.95≤ m ≤1.05 for category 1 elements, while m ≤0.95 or m ≥1.05 for category 2 elements. Category 2 elements should be corrected with a post-collection data calibration.

Elements in category 3 (As and Cu), have lower precision and slopes far from 1 (RSD <5%, m ≤0.95 or m ≥1.05), but still produce highly linear results ($R^2$ >0.97). Calibration should improve the accuracy of their data, but they may still be less precise than elements in categories 1 or 2. An element could potentially be in this category and possess a RSD much greater than 5%, in this case repeated analyses would be necessary to obtain reliable pXRF data.

Elements in category 4 have slopes close to one (0.95≤ m ≤1.05), however they either have less linear results (Ba, Ti, Cr), and/or are measured less precisely (Pb, Cr). Calibrating these elements can only provide minor improvements, perhaps with the exception of Ti, which has a slope close to one, but its y-intercept is high (y = 0.999x + 244). It should be noted that Ba, Cr, Pb and Ti nearly meet conditions to be in category 1, and can be effectively analysed with the pXRF with minor precautions.

Elements of category 5 have low precision (RSD >5%), low linearity ($R^2$ <0.97), and m ≤0.95 or m ≥1.05, for the sample matrices and concentration levels analysed. Cs does not show any linearity since the concentrations near or below the reported detection limit of 35 ppm for a $SiO_2$+Fe+Ca matrix material is (Thermo Scientific, 2008). Th displays more precise results than others in category 5, but has little linearity ($R^2$ = 0.6269) and a slope of 2.09. However, all Th concentrations are below 20 ppm, so samples with higher concentrations (and a larger range of concentrations) would likely improve all three statistics. The reported detection limit for Th in a $SiO_2$+Fe+Ca matrix material is 4 ppm (Thermo Scientific, 2008). Ni shows similar linearity ($R^2$

= 0.5890) to Th, but little precision. As with Th, it should be noted that all the Ni concentration are below 50 ppm (detection limit for a $SiO_2$+Fe+Ca matrix material of 30 ppm) and its %RSD is likely much lower for higher concentrations, but even at higher concentrations it is difficult to detect accurately. For example, Ni From NIST 610 with a 60 second dwell time returns a mean concentration of 770 ppm for 111 analyses (Appendix A and B) where the recommended value is much lower at 459 ppm. For DLH 10b determination of Ni with a 60 second dwell time returns a mean concentration of 546 ppm for 115 analyses (Appendix A and B) where the recommended value is much higher at 928 ppm. However, note again these are all glass standards and not soils, and the results may be due to matrix issues. To achieve accurate results for Ni it is especially important to analyses standards that are similar to the materials being examined.

The 14 elements in categories 1 to 4 (As, Ba, Ca, Cr, Cu, Fe, K, Mn, Pb, Rb, Sr, Ti, Zn, and Zr) produce acceptable results without calibration, however post-collection data correction utilizing calibration curves of category 2 and 3 elements should improve results. V may also produce acceptable results with repeated analysis, although a post-collection data correction would be necessary.

## 6.0 Conclusion

The Niton XL3t GOLDD XRF spectrometer with a Cygnet 50 kV X-ray tube collecting data in Soil Mode can be an effective tool in determining the concentrations of about 14 elements in five siliciclastic sediments utilizing the factory calibration. While collecting data with the pXRF it is vital to run both a recognized set of reference standards with recommended values and a suite of in house standards linked directly to the material being analysed. Interestingly, the pXRF spectrometer was effective in determining many—but not all—elements in four glass standards, with a matrix that is distinctly non-soil-like.

For all standards, acquiring data with dwell times below 30 seconds per filter, in general did not provide precise results. However, analyzing a sample for long periods of time (>70 seconds) may result in saturation of the detector and produce erroneous values. For many elements and for most concentration ranges, we suggest dwell times of no less than 30 seconds or not greater than 60 seconds is optimal. However, longer dwell times are required for elements that have concentration levels near the limit of detection.

Most elements display some variation in measurements over time that may be attributed to instrumental drift, however many of these variations are within the data's uncertainty limits. Thus, the pXRF does not display instrumental drift for most of the elements analysed. Drift can be monitored by examination of several elements such as U, which may provide insight into more subtle drift recorded by other elements (e.g. K, Ca). Peak interferences and subsequent deconvolution of the spectra represent one of the limitations of the pXRF method. Moreover, the long-term elemental concentration variation observed for some elements (e.g., Ca and K) effectively decreases precision and complicates the interpretation of data sets collected over the

period of months. Decreased precision is also highly affected by dwell times lower than 30 seconds, whereas improved precision is rarely observed for dwell times ≥40 seconds.

Examination of Till-1, -2, -3, and -4 has demonstrated that calibration of the spectrometer is not always necessary, but is often beneficial for elements at very high, or low, concentrations. For those elements with unsatisfactory accuracy using the factory calibration, data may be post-acquisition processed (i.e., using a calibration based on analysis of standards) to provide more accurate results. Although satisfactory results can be determined by the pXRF spectrometer in soil mode on glass matrix reference materials, we recommended that a series of reference materials with a matrix similar to that of the samples being examined be analyzed after approximately every 10 analyses.

The data tables compiled in this report provide a broad range of analyses of reference materials that encompass from both low and high elemental concentrations and various dwell times that can be used to compare to future analyses of the same reference materials used as a standard in research activities.

## Acknowledgments

We thank Pierre Pelchat and Gwendy Hall (retired) of the GSC for many insights about the nuances of pXRF spectrometers. Critical review was carried out by Christopher Lawley and Katherine Venance. This study was undertaken and supported by the Target Geosciences Initiative (TGI-4) Method Development Project, Geomapping for Energy and Minerals (GEM) Diamond Project, and the Aquifer Assessments and Support to Mapping: Groundwater Inventory, Groundwater Geoscience Program, at the Geological Survey of Canada.

## References


Crow, H. L., Knight, R. D., Medioli, B. E., Hinton, M. J., Plourde, A., Pugin, A. J.-M., Brewer, K. D., Russell, H. A. J, and Sharpe, D. R., 2012. Geological, hydrogeological, geophysical, and geochemistry data from a cored borehole in the Spiritwood buried valley, SW Manitoba. Geological Survey of Canada, Open File 7079, 31 p.

Gazley, M.F., Vry, J.K., du Plessis, E., Handler, M.R. 2011. Application of portable X-ray flourescene analyses to metabasalt stratigraphy, Plutonic Gold Mine, Western Australia. Journal of Geochemical Exploration, v. 110, p. 74-80.

Girard, I., Klassen, R.A., and Laframboise, R.R., 2004. Sedimentology laboratory manual, terrain sciences division. Geological Survey of Canada, Open File 4823, 134 p.

Goldstein, J.I., Newbury, D.E., Echlin, P., Joy, D.C., Roming Jr, A.D., Lyman, C.E., Fiori, C. and Lifshin, E. 1992. Scanning Electron Microscopy and X-ray Microanalysis: a Text for Biologists, Materials Scientists, and Geologists, 2nd edition. Springer, 820.p.

Grunsky, E. C., Kjarsgaard, B.A., Kurszlaukis, S., Seller, M., Knight, R.D. and Moroz, M. 2013. Classification of whole-rock geochemistry based on statistical treatment of whole-rock geochemical analyses and portable XRF analyses at the Attawapiskat Kimberlite Field of Ontario. Geological Survey of Canada, Scientific Presentation 15, 2013; 1 sheet, doi:10.4095/292446

Hamilton, D.L. and Hopkins, T.C., 1995. Preparation of glasses for use as chemical standards involving the coprecipitated gel technique. Analyst, v. 120, p. 1373-1377.

Hinton, R.W., 2007. NIST 610, 611 and SRM 612, 613 Multi-element glasses: constraints from element abundance ratios measured by microprobe techniques. Geostandards Newsletter, Journal of Geostandards and Geoanalysis, v. 23, n. 2, p. 197-207.

Jochum, K.P., Weis, U., Stoll, B., Kuzmin, D., Yang, Q., Raczek, I., Jacob, D.E., Stracke, A., Birbaum, K., Frick, D.A., Günther, D., and Enzweiler, J., 2011. Determination of reference values for NIST SRM 610-617 glasses following ISO guidelines. Geostandards and Geoanalytical Research, v. 35, n. 4, p. 397-429.

Kenna, T.C., Nitsche, F.O., Herron, M.M., Mailloux, B.J., Peteet, D., Sritrairat, S., Sands, E., and Baumgarten, J., 2011. Evaluation and calibration of a Field Portable X-Ray Fluorescence spectrometer for quantitative analysis of siliciclastic soils and sediments. Journal of Analytical Atomic Spectrometry, v. 26, p. 395-405.

Kjarsgaard, B.A., Knight, R., Grunsky, E., Kerr, D., Sharpe, D.R., Cummings, D.I., Russell, H.A.J., Wright, D., 2013 (in press). Till geochemistry studies of the East Arm MERA study area. Geological Survey of Canada, Open File.

Knight, R.D., Moroz, M., and Russell, H.J.A., 2012. Geochemistry of a Champlain Sea aquitard: portable XRF analysis.Geological Survey of Canada, Open File 7085, 35 p.

Lynch, J., 1996. Provisional elemental values for four new geochemical soil and till reference materials, TILL-1, TILL-2, TILL-3 and TILL-4. Geostandards Newsletter, v. 20, n. 2, p. 277-287.

McLaren, T.E., Guppy, C.N., Forster, N., Grave, P., Lisle, L.M., and Bennett, J.W. 2011. Rapid, non-destructive total elemental analysis of Vertisol soils using portable X-ray fluorescence. Soil Society of America Journal, v. 76, p. 1436-1445.

Morris, P.A., 2009. Field-portable X-ray fluorescence analysis and its application in GSWA. Geological Survey of Western Australia, Record 2009/7, 23p.

Pearce, N.J.G., Perkins, W.T., Westgate, J.A., Gorton, M.P., Jackson, S.E., Neal, C.R., and Chenery, S.P. 1997. A compilation of new and published major and trace element data for NIST SRM 610 and NIST SRM 612 glass reference materials. Geostandards Newsletter, Journal of Geostandards and Geoanalysis, v. 21, n. 1, p. 115-144.

Plourde, A.P., Knight, R.D., Russell, H.A.J. 2012. Portable XRF spectrometry of in-situ and processed glacial sediment from a borehole within the Spiritwood buried valley, southwest Manitoba. Geological Survey of Canada, Open File 7262, 30 p.

Radu, T. and Diamond, D. 2009. Comparison of soil pollution concentrations determined using AAS and portable XRF techniques. Journal of Hazardous Materials, v. 171, p. 1168-1171.

Rowe, H., Hughes, N., and Robinson K., 2012. The quantification and application of handheld energy-dispersive x-ray fluorescence (ED-XRF) in mudrock chemostratigraphy and geochemistry. Chemical Geology, v. 324, p. 122-131.

Stanley, G., Gallagher, V., NiMhairtin, F., Brogan, J., Lally, P., Doyle, E., Farrell, L., 2009. Historic mines site inventory and rick classification. Geochemical characterization and environmental matters, Geological Survey of Ireland v.1, Appendix 4-XRF analyser, Assessment of analytical performance of Niton XLt 792Y field-portable analyser, 40 p.

Thermo Scientific, 2008. Elemental limits of detection in $Si0_2$ and SRM matrices using soil analysis. Niton XL3t GOLDD + Series x-ray fluorescence analyzer spec sheet.

Weindorf, D.C., Zhu, Y., Chakraborty, Somsubhra, Bakr, N. and Huang, B. 2012. Use of portable X-ray fluorescence spectrometry for environmental quality assessment of peri-urban agriculture. Environmental Monitoring and Assessment, v.184, p. 217-227.

Weltje, G.J. and Tjallingii, R., 2008. Calibration of XRF core scanners for quantitative geochemical logging of sediment cores: theory and application. Earth and Planetary Science Letters, v. 274, p. 423-428.

Wilson, S.A., Briggs, P.H., Brown, Z.A., Taggart, J.E. and Knight, R., 1999. Collection, preparation and testing of NIST hard rock mine waste reference material SRM 2780. USGS Open File Report 99-370, 15 p.